Scilight

Renewable and Sustainable Energy Technology

https://www.sciltp.com/journals/rset

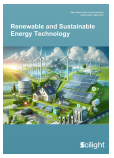

Review

Graphitic Carbon Nitride, Synthesis Strategies, Characteristics and Application as an Electrode for Advanced Rechargeable Battery Systems

Qaisar Abbas [1,*], Pragati A. Shinde [2], Mohammad Ali Abdelkareem [3], Rizwan Raza [4] and Abdul Ghani Olabi [3,*]

[1] Institute of Thin Films, Sensors and Imaging (ITFSI), School of Computing, Engineering and Physical Sciences, University of The West of Scotland, Glasgow PA1 2BE, UK
[2] Research Center for Materials Nanoarchitectonics, National Institute for Materials Science (NIMS), 1-1 Namiki, Tsukuba 305-0044 Japan
[3] Sustainable Energy & Power Systems Research Centre, RISE, University of Sharjah, Sharjah P.O. Box 27272, United Arab Emirates
[4] Clean Energy Research Lab (CERL), Department of Physics, COMSATS University Islamabad, Lahore Campus, Lahore 54000, Pakistan
* Correspondence: qaisar.abbas@uws.ac.uk (Q.A.); aolabi@sharjah.ac.ae (A.G.O.)

How To Cite: Abbas, Q.; Shinde, P.A.; Abdelkareem, M.A.; et al. Graphitic Carbon Nitride, Synthesis Strategies, Characteristics and Application as an Electrode for Advanced Rechargeable Battery Systems. *Renewable and Sustainable Energy Technology* **2025**. https://doi.org/10.53941/rest.2025.100009

Received: 25 March 2025
Revised: 2 September 2025
Accepted: 3 September 2025
Published: 10 September 2025

Abstract: Electrochemical energy storage devices, particularly widely used rechargeable batteries, have attracted immense interest due to maturity in technology, ease of adaptability, technological diversity, superior energy density, high conversion efficiency and extensive accessibility of these systems. This has resulted in diversification of commercial applications of these devices ranging from portable consumer electronics to transportation. Less hazardous and abundant cell components are crucial for further broadening of their applicability for largescale applications such as grid-scale storage in a cost-effective and environmentally friendly manner. Electrode is a vital component of any battery systems and can significantly impact its performance. Therefore, it is imperative to investigate different electrode materials for leading rechargeable batteries. Key motivation of this study was to evaluate graphitic-C_3N_4 as a potential electrode material for advanced rechargeable battery systems since it is considered both cost-effective and environmentally friendly. Moreover, a two-dimensional layered structure of graphitic-C_3N_4 which is analogous of graphene has potential to enhance the energy storage performance of rechargeable batteries. During this study various synthesis strategies to produce graphitic-C_3N_4, with their advantages and disadvantages have been discussed. It's application as an electrode material particularly for advanced/futuristic battery systems based on lithium-ion, lithium sulfur, sodium-ion and metal air batteries have also been covered comprehensively which makes this work rather distinctive. This study concluded that graphitic-C_3N_4 has immense potential to be an active material for battery systems. However, further work is required to optimize it's structure, surface chemistry and hybridization with other promising active materials.

Keywords: energy storage; advanced rechargeable batteries; electrode materials; graphitic carbon nitride; synthesis strategies

1. Introduction

Rechargeable batteries (RB) technology has evolved over the past century and has become an integral part of modern society by distributing electrical energy on demand for a multitude of everyday applications. Pioneering advancements in the field of RB technology throughout the 20th century, with acceleration in developments of lithium-ion batteries (LIB) in mid-80's has led to strong research and development in this area in the last three decades [1–4]. For years, LIBs maintained dominance in the RBs market since portable consumer electronic devices were considered the key driving force behind this demand. However, step changes in these applications have been observed with two vital research areas coming into the spotlight. Firstly, after several failed attempts, electric and hybrid electric vehicles (EVs/HEVs) have finally reached mass production stage during the last few years making it the single largest consumer market segment of large-scale battery systems. Secondly, renewable energy predominantly based on solar and wind has grown exponentially over the past few years [5–7]. It is anticipated; further incorporation of these green sources requires grid scale electrical energy storage to store additional power generated through renewable using low cost RBs. It is also predicted that innovations in other areas including robotics and miniaturized smart devices will gain more relevance in coming years making thin film-based batteries highly desirable. Requirements of these newly emerging applications are diverse; no single battery type can fulfil these requirements. Therefore, different battery chemistries are being developed with focus on LIBs and sodium-ion batteries (NIBs) [8–10]. Furthermore, new types of battery chemistries and cell designs will be necessary to fulfil the energy requirements of these ever-evolving applications. There is particular emphasis on the development of solid-state batteries systems for enhanced safety and increased potential of recycling [11].

Significant progress has been made in recent years to optimize various components of a battery system such as electrolyte, current collectors, cell design and electrode materials to further enhance battery performance. Electrode is a fundamental component of any battery system, governing the battery performance in terms of lifespan, safety, cyclability and energy storage capacity [12]. Diverse ranges of electrode materials have been developed for both LIBs and NIBs with keeping in mind vital characteristics such as, cost, scalability, safety, availability and environmental impact. These electrode materials can be classified into two broader groups i.e., intercalation and conversion electrode materials where these materials have their own advantages and disadvantages. For LIBs, $LiCoO_2$ [13], $LiFeO_4$ [14], $LiMn_2O_4$ [15], $LiNi_{0.8}Co_{0.1}Mn_{0.1}O_2$ (NCM811) [16], $LiNi_{0.8}Co_{0.15}Al_{0.05}O_2$(NCA) [17], and graphite [18] are considered state of the art intercalation type electrodes. In intercalation electrode, Lithium ions reversibly intercalate/de-intercalate without a considerable volume change, exhibiting a stable cycling but have inferior specific capacity. Whereas metal sulphides [19], halides [20] and oxides [21] can be grouped as conversion electrodes. In conversion electrodes, the charge-discharge process is complemented by phase transition during conversion reaction resulting in much higher capacity but have poor cycling (due to structural breakdown) and reversibility issues. Whereas in case of NIBs, carbon-based nanostructures [22] and Ti-based oxides [23] and their composites [24] are typical materials developed on the basis of intercalation reaction mechanism. Likewise, metal sulphides [25], selenides [26], halides [27], oxides [28], phosphides [29], nitrides [30] and fluorides [31] are conversion types of electrode materials thanks to their cost-effectiveness and superior theoretical capacity [32,33].

Among the wide range of electrode materials (few mentioned above), carbon nanomaterials particularly graphite are highly desirable since they are considered the most promising due to their distinctive characteristics' such as natural abundance, good conductivity, high chemical stability, low cost, small volume changes, flat voltage range and ease of processibility. These carbon-based electrodes are further hybridized with transition metals to improve both storage performance as well as cyclability and electronic conductivity. A recent study by Ma, Yuan, et al., showed successful incorporation of CoS_2 nanoparticles within the porous carbonaceous micro-polyhedrons, interwoven with CNTs. This not only resulted in superior electronic conductivity but also delivered superior energy storage performance of 1030 mAh g^{-1} after 120 cycles and 403 mAh g^{-1} after 200 cycles (at 100 mA g^{-1}) as electrode for lithium-ion (LIBs) and sodium-ion batteries (SIBs), respectively [34]. Another challenge carbon-based electrodes, particularly hard carbon faces, is the accommodation of sodium-ions due to highly restrictive porous structure and smaller interlayer spacing where different strategies have been devised to address. Zinc assisted strategy where this strategy not only optimizes the porous structure but also increases the interlayer spacing to accommodate larger sized sodium-ions [35]. Transition metal oxides are another potential anode materials for batteries however these nanomaterials suffer from low electronic conductivity and large volume changes. Numerous strategies have been devised to address these shortcomings where one of the key strategy is carbon coating and heteroatoms doping [36]. Moreover, Nitrogen functionalised carbons i.e., graphitic carbon nitride (graphitic-C_3N_4) have attracted great consideration due to its edge N defects (pyridinic N and pyrrolic N), especially for the case of SIBs since these defects can accommodate the adsorption and diffusion of sodium ions

and thus improve sodium storage capacity and rate capability [37]. Graphitic-C_3N_4 has been seen as a potential electrode material for rechargeable battery systems, a highly reversible capacity of 2753 mAh g^{-1} was realised after the 300th cycle with improved cycling stability and rate capability when controlled nitrogen content (using magnesiothermic denitriding technology) g-C_3N_4 was used as an anode. Similarly for LIBs, graphitic-C_3N_4 which is essentially a nitrogen doped graphene with higher nitrogen content has displayed enhanced lithium storage capacities [38]. A study by Gope, Subhra et al., where graphitic-C_3N_4 use pyrolysis thiourea route to produce and was used as an anode in LIB for full cell. As can be witnessed, graphitic-C_3N_4 retains much superior performance as compared to conventional carbon electrode. The capacity of 92 mAh g^{-1} with the stabilized capacity retention of around 95% [39]. Furthermore, the presence of nitrogen presents another advantage in terms of chemical composition and edge N defects resulting in improved performance. Due to these reasons, it can be presumed that graphitic-C_3N_4 can be used as an effective alternative of traditional carbon/noncarbon anodes for LIBs. Lithium sulfur batteries is another class of futuristic rechargeable battery systems which has sought attention lately due to it exceptionally high theoretical capacity and energy density of 1675 mAh g^{-1}) and 2600 Wh kg^{-1} respectively [40]. A recent study by Sun, Wenhao, et al. has shown that outstanding discharge capacity of 471 mAh g^{-1} was achieved after 400 cycles with very low fading rate in capacity of 0.030% when a layer of graphitic-C_3N_4 was applied on the anode.

Over the past decade, graphitic-C_3N_4 seemed to have drawn increased interest as an electrode for wide range of rechargeable batteries. Figure 1 shows the statistical data in terms of number of publications over the past ten years (from 2014 to 2023) where the inset shows the type of publications during this period when graphitic-C_3N_4 is used as a battery electrode. Steady growth can be viewed over the period with this growth acceleration substantially in the past five years. Moreover, on the detailed analysis of the type of publications, it is evident that experimental research articles are the major category symbolising the experimental work while using graphitic-C_3N_4 as an electrode in rechargeable battery segment.

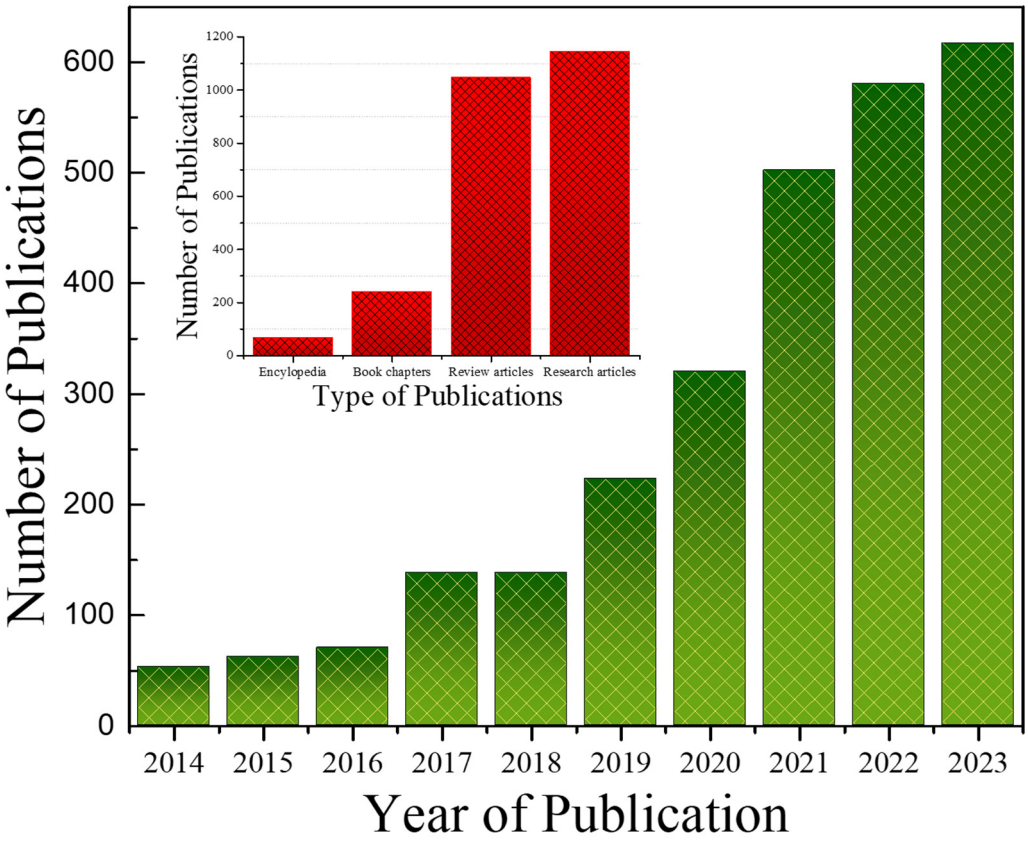

Figure 1. Statistical data analysis of number of publications on graphitic-C_3N_4 in the past 10 years (inset figure illustrates the statistical data analysis of type of publications same period).

This review article covers up-to-date progress on state-of-the-art synthesis techniques used to produce graphitic-C_3N_4. Followed by its distinct properties and applications as an electrode in advanced rechargeable batteries (commercialised or in research phase) i.e., lithium-ion, sodium-ion and lithium sulfur and metal air batteries. Finally, the prospect of this nanomaterial (stand alone, it's derivates or a composite) in terms of its use

as electrode in electrochemical applications in general and in current/futuristics rechargeable battery applications in particular has been covered in detail.

2. Synthesis Strategies for Graphitic-C_3N_4

Normally, the production process of graphitic-C_3N_4 can be divided into two phases i.e., polyaddition and polycondensation. During the polyaddition process, precursor is polymerised to melamine. This is followed by polycondensation during which melamine is converted to graphitic-C_3N_4 with the loss of ammonia while both of these processes are template dependent [41]. Precursors including melamine, urea, dicyandiamide, thiourea and cyanamide are thermally polymerised to synthesise g-C_3N_4. Various structural characteristics such as pore volume, surface area and grain size can impact physiochemical and electrochemical properties of graphitic-C_3N_4 [42–44]. Therefore, variety of production processes have been developed to fine-tune these characteristics and synthesis strategies [45,46]. Employed precursors, state of the art synthesis procedures and distinctive properties of graphitic-C_3N_4 are depicted graphically in Figure 2. It can be witnessed that large number of synthesis procedures are used to produce graphitic-C_3N_4. In the following subsections some of the most commonly used synthesis procedures such as templating method, sol-gel method, supramolecular self-assembly and exfoliation method will be discussed. The properties of produced graphitic-C_3N_4 and advantages/disadvantages of the production process will also be discussed briefly.

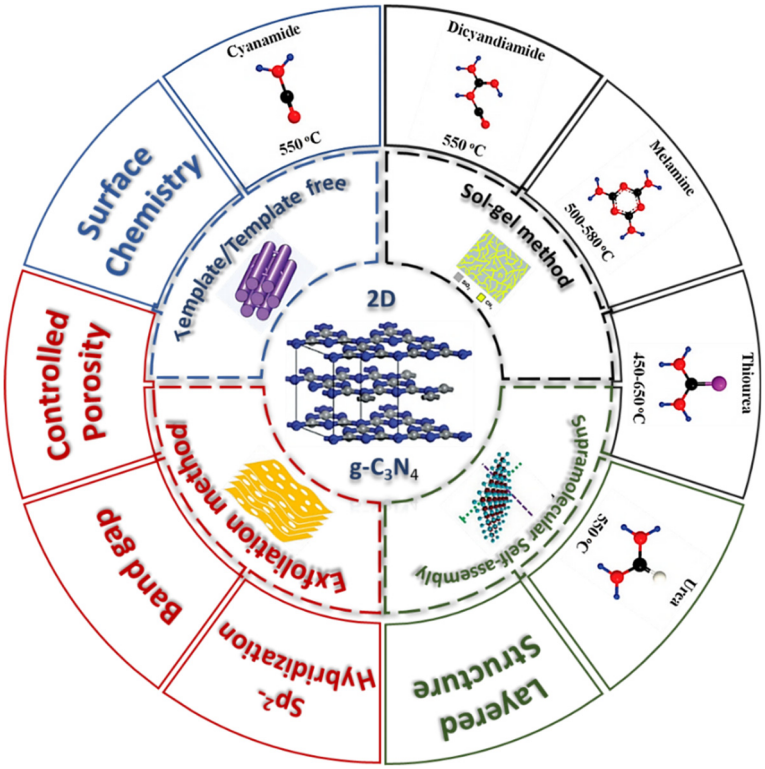

Figure 2. Graphical illustration of synthesis strategies, precursors and distinct characteristics of graphitic-C_3N_4.

2.1. Templating Method

Templating is a facile and effective method where both soft and hard templates are used during this production process. We will briefly describe this process along with properties optimisation using this technique during this section. Advantages of templating methods include the control over porous structure, size, and overall morphology where the architectures of the produced samples directly relate to the design of the template used [47–49]. Uniform porous structure, excellent design, ease of detachability and chemical innerness are some of the properties required for an ideal template material. Groundbreaking work to produce graphitic-C_3N_4 using hard template was reported in 2005 by Groenewolt and co-workers where porous silica was used as a host matrix [50]. Immense amount of research activity has been guided towards the synthesis of graphitic-C_3N_4 using hard template method. This method can be broadly divided into three key steps: (1) selection and preparation of suitable hard template; (2) coating of precursor of targeted material on to the hard template; (3) disintegration of hard template [51,52]. Nanocoating is commonly used to precisely coat the precursor to load the hard template. Appropriately, size, porous structure and the morphology of the produced graphitic-C_3N_4 can be accurately controlled in relative to the used hard template.

Crystallinity and planner atomic structure is not impacted due to the chemical inertness of these used hard templates. Hard template method has got a great potential to provide control over porous structure of resulting graphitic-C_3N_4. However, the complexity of this process coupled with association of extremely toxic removers make it less desirable. Therefore, further research is required to make this method greener and more facile [53]. Thanks to its facile preparation process and the absence of template removal, soft template has become an attractive choice [54,55]. Most frequently used soft template methods include bubble and surfactant methods. During this simpler process the templates will self-remove itself during the synthesis reaction [56]. However, soft template has not been as vigorously investigated as hard template method therefore has limited number of procedures when compared to hard template method. Discovery of new soft templates is therefore necessary to make it more useful and widespread. Moreover, in some instances control of properties of produced graphitic-C_3N_4 is not as precise as hard template therefore its areas of applications are also restricted.

2.2. Sol-Gel Method

Sol-gel method is another popular procedure which can be used to produce graphitic-C_3N_4 where the precursor of graphitic-C_3N_4 is mixed with the precursor of silica or a sol of silica [57]. During the preparation of graphitic-C_3N_4 using so-gel method hard template is also used however this template is not pre-synthesised as in the case of hard templating but both production and removal of template based on silica is performed during the synthesis reaction [58,59]. Using the sol-gel approach to produce graphitic-C_3N_4, the precursors and subsequently the composites can be processed into monoliths and thin films, resulting in broadening their applications. Once again using sol-gel method involves template which require removal making this process complicated [60,61].

2.3. Supramolecular Self-Assembly

Supramolecular self-assembly is another production process which can be used to produce graphitic-C_3N_4 by employing both single precursor and multiple precursors synthesis strategies. In typical single precursor supramolecular self-assembly, melamine is the most commonly used precursor and cyanuric acid as a solvent since melamine is capable of forming π-π and hydrogen bonding interactions. However, it is quite difficult to dissolve melamine in cyanuric acid to produce graphitic-C_3N_4. Therefore, attention has been focused on exploring alternative solutions both acidic and basic solutions such as HCL and NaOH respectively have been widely explored to dissolve melamine [62,63]. To effectively dissolve melamine in acidic solution, a hydrothermal process has been adopted, followed by the pyrolysis process to form the graphitic-C_3N_4 structure as shown Figure 3a,b. To improve the morphological control of produced graphitic-C_3N_4 apart from single precursor, multiple precursors supramolecular self-assembly synthesis strategy is considered highly desirable. Since, the self-assembly during single precursor process involves precursor and partially hydrolysed analogue where the uncertainty over the degree of hydrolysis confines the control over self-assembly thereby losing control over the physio-chemical characteristics of produce graphitic-C_3N_4 [62,64]. Control over morphology and textural architects are mainly determined by the direction of hydrogen bonds and π–π interaction between the monomer units. Quantitative control over the monomer units controls the physical property such induced defects and chemical characteristics such as level of heteroatom functionalisation and nitrogen-to-carbon ratio which can be controlled with ease using multiple precursor method. Highly stable Plate-like morphologies and aggregated co-crystal were reported whereby mixing equimolar solutions in Dimethyl sulfoxide, water and chloroform solvents melamine–trithiocyanuric acid supramolecular complex is formed [65] as shown in Figure 3c. The formation of these stable aggregate structures determined the final structure of the compounds.

2.4. Exfoliation Method

Exfoliation method is a vital technique to fine-tune the physical and chemical characteristics such as surface area, pore size and conductivity of graphitic-C_3N_4, where produced graphitic-C_3N_4 commonly displays stalked layered structure comprised of nanosheets. There are number of exfoliation techniques however ultra-sonication [66], oxidation etching [67], thermal calcination [68] and combination of thermal calcination and ultra-sonication [69] are the commonly used processes. Among other exfoliation techniques liquid phase exfoliation has received considerable attention since it simpler and cost-effective [70]. In a recent study, graphitic-C_3N_4 was prepared using inexpensive precursor based on urea in water assisted by sonication with varied timescales while using sonication frequency of 60 Hz. Synthesis of graphitic-C_3N_4 carried out at room temperature and pressure and schematic of production process has been displayed in Figure 3d [71].

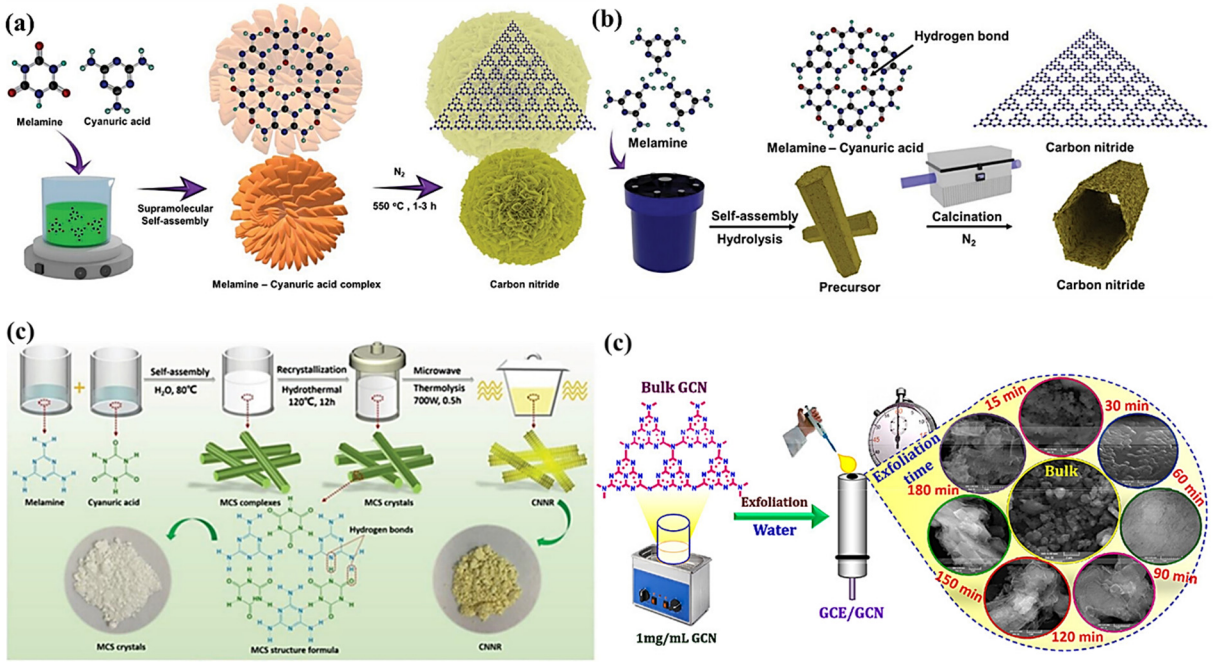

Figure 3. Various synthesis routes to produce graphitic-C_3N_4 (**a**) schematic of the synthesis based on supramolecular self-assembly single precursor route, (**b**) graphical presentation of the production of graphitic-C_3N_4 based on melamine using hydrothermal synthesis route, (**c**) schematic illustration of the multiple precursors synthesis strategies based on supramolecular self-assembly method and (**d**) schematic displaying the sequential exfoliation of graphitic-C_3N_4 in water assisted by sonication at different time intervals [71–73].

In summary, every synthesis procedure has its own advantages and disadvantages depending on cost, complexity, properties of produced graphitic-C_3N_4 and environmentally friendliness. Level of control over morphology, physical and chemical characteristics varies with each method. Therefore, desired physiochemical properties can be modulated through the selection of appropriate process based on the intended application. Furthermore, during large scale production of graphitic-C_3N_4, restacking of individual 2D layers can be an immense challenge which can not only impact the overall material's porous structure but can also influence its electrochemical performance. Therefore, production of composites/hybrid using highly conductive materials such as MXenes, transition metal oxides and conducting polymers can assist in avoiding restacking of individual layers. This will improve the 2D networks and therefore porosity of the materials which can increase the electrochemically active sites and ultimately the performance of electrochemical energy storage/conversion devices.

3. Brief History of Rechargeable Batteries (RBs)

At present, LIBs are considered the market leader and unanimously acclaimed as the face of rechargeable battery technology whereas this technology had only been developed in past few decades. However, RB technology goes back in history more than a century with the lead-acid batteries being the pioneering systems which still remains the leading battery system with the commercial applications spanning over 160 years [74]. Even though, its utilization in newly emerging applications is limited due to its, limited cyclic performance and high maintenance together with inferior energy storage capability where the average energy density of the cell lingering somewhere between 30–40 Wh kg^{-1}. However, exceptional cost-effectiveness of lead-acid batteries and maturity of technology make these systems highly desirable for traditional applications particularly in transportation as starting batteries such as in cars, mobility vehicles, golf carts. It is anticipated that these batteries will retain their market share in segments where other batteries are considered too expensive. Nickel-cadmium (Ni-Cd) batteries were the next class of rechargeable batteries to be developed. These batteries were first conceptualised in 1901 by EW Jungner and becomes commercially available much later [75]. Ni-Cd batteries became commercial success much later in 1947 with the development of less expensive nickel electrodes. These batteries found number of applications in portable accumulator market including power tools and early mobile phones due to much superior performance characteristics such as enhanced cyclic performance and superior energy density of between 40–60 Wh kg^{-1} [76]. However, Ni-Cd batteries have number of fundamental flaws i.e., toxicity associated with cadmium, thermal runaways and infamous memory effect which made these systems less desirable overtime [77,78]. Market share of Ni-Cd batteries nearly diminished over time with the exception of some very

niche applications. This was particularly affected by the emergence of Ni-MH batteries where newly developed electrochemistry of these batteries allowed to attain much superior energy densities which were not realisable using older technology-based lead-acid or Ni-Cd batteries. Overall, stable long-term performance, excellent safety and comparatively lower cost made Ni-MH batteries popular choice for earlier generation of electric vehicles [79]. Ni-MH batteries replaced Ni-Cd battery systems swiftly in number of other industrial applications as well. Ni-MH batteries seen diversification in their application base with wider use in newly developed consumer electronics to large scale applications such as electric/hybrid electric vehicles. These RBs were initially used in 1st generation hybrid and all electric vehicles including Toyota Prius and GM EV1& Honda EV Plus respectively [2,80]. However, this commercial success was short lived, these systems were squeezed out from vehicle segment of the market with the emergence of LIBs. However, these batteries are still available as small rechargeable systems and also used in some hybrid electric vehicles to reduce cost [81].

State of the art battery technology currently known as LIBs, gained public interest in mid 80s and has had wide ranging transformational impact on people particularly on communication, personal electronics, entertainment, transportation, information. In more recent past, it has unprecedently influenced and tailored our lifestyle through portable information and communication technology [10,82,83]. It has unparalleled impact on two key fronts i.e., entertainment/communication and transportation. Miniaturization is the crucial factor in former category since portable electronics such as cellular phones, handheld music players has resulted in improved communication/networking and has relandscaped the music seen. Similar transformation has also taken place in transportation sector with large scale manufacturing of electric/hybrid electric vehicles in past couple of decades [84–86]. Similar revolutions are anticipated in energy sector with the wider deployment of renewables sources based on solar, wind and tidal where large energy storage will be vital to address the intermittency of these resources. It has also been predicted that the underlying technology of LIBs might have reached its saturation point. A major breakthrough is necessary for further development of this technology or alternative battery technology/chemistry is obligatory. Cost of lithium makes it unsuitable for large scale application which is affected by supply/demand imbalance and uneven geographical distribution which adds enormous transportation cost.

Sodium has been considered a suitable substitute due to its similar physiochemical properties and earth abundance. NIBs can hold significant promise for future transportation requirement and grid scale energy storage as large number of studies have cemented the viability of these electrochemical energy storage devices for both stationary and mobile commercial applications [87–90]. Development of NIBs was carried out in parallel to LIBs, however with the success of LIBs thanks to the discovery of natural graphite as a suitable anode material coupled with failure to intercalate sodium ions (due to larger ion size) restricted the development of these battery systems. Research on NIBs picked up pace once again with the possibility of using hard carbon to deliver energy storage capability similar to those of LIBs [91,92]. Alternative way to substitute or complement LIBs is to development new chemistries where higher level of energy can be stored in similar mass or volume to have high gravimetric or volumetric energy storage respectively. To accomplish this, materials with higher theoretical energy storage ability should be investigated. Lithium sulfur batteries (LISBs) are considered a suitable candidate for these applications since they are able to deliver much higher theoretical capacity of 1675 mAh g^{-1} and specific energy of 2600 Wh kg^{-1} [93,94]. Furthermore, these batteries are inexpensive, better cyclic life, safer and environmentally less harmful [95]. Figure 4 shows the comparison between different battery technologies in terms of both gravimetric and volumetric energy densities.

Among other electrode materials, graphitic-C_3N_4 has seem immense interest as active materials in rechargeable batteries. graphitic-C_3N_4 is fundamentally a stack of one-atom-thick planar sheets of sp^2 hybridized carbon and nitrogen atoms, has promising electrical, optical, structural, and physiochemical properties together with low-cost availability [96,97]. In the following subsections, applications of graphitic-C_3N_4 as an electrode in advanced RBs will be discussed in detail.

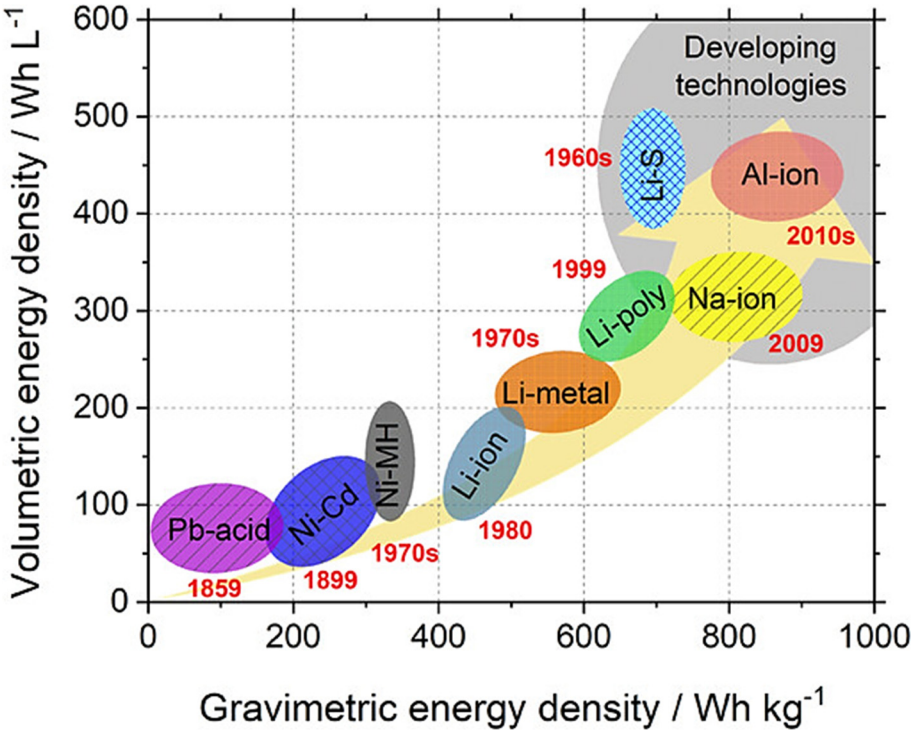

Figure 4. Comparison of different battery technologies in terms of their volumetric/gravimetric energy density [2].

4. Graphitic Carbon Nitride (g-C_3N_4) for Battery Applications

As discussed previously, research field of rechargeable batteries is exceptionally broad and thriving at fast pace, backed by immense scientific research drive to keep up with accelerated introduction of new and innovative battery applications including medical implants, EVs/HEVs, satellites, portable electronics, and drones [98–100]. The introduction of new electrode, electrolytes and membrane materials has resulted in enhancement in battery performance coupled with reduction in prices and versatility in battery's cell designs/sizes particularly lithium-ion batteries (LIBs) [101]. Forecasting of future battery chemistries and availability of raw materials are some of the fundamental questions required answering. Currently, LIBs are leading the way due to the improvements in their power capability, energy density, and reduction in overall cost of manufacturing over past three decades. However, safety and mounting material cost are key concerns for these battery systems. Attempts are being made to address safety concerns by developing solid state batteries and improved separator technology. Issue of cost being delt with by developing alternative battery chemistries such as sodium-ion (SIBs) and metal air batteries (MABs) [102,103]. To improve the energy storage capabilities and reduce cost even further new battery chemistries such as lithium sulfur batteries (LSBs) are being developed [93,104,105]. New and novel electrode materials such as graphene, carbon nanotubes, MXenes, metal organic framework and graphitic-C_3N_4 are being developed and deployed in these newly emerging battery chemistries [106–109]. Electrode is a vital component of any battery system and graphite is commonly used in most of the battery systems. However, graphite has limited theoretical capacity of around 372 mAh g^{-1} restricting the overall capacitive performance of a battery [110]. In this section we will endeavour to evaluate graphiric-C_3N_4 and its hybrids as electrode in different batteries including LIBs, SIBs and LSBs and MABs.

4.1. Lithium Sulfur Batteries (LSBs)

LSBs have gained researcher's attention recently due to their outstanding performance characteristics such as high theoretical energy density of up to 2600 Wh kg^{-1} (around 10 times higher than those of commercialized LIBs with theoretical energy density of 265 Wh kg^{-1}), low cost, superior capacities and improved safety [111]. However, commercialization of LSBs has been hampered by number of impediments. Some of the key obstacles include the inferior rate performance and un-efficient use of electrode surface area which is caused by low electronic conductivity (10^{-15} S m^{-1}) and aggregation of sulfur and its intermediates (Li_2S, Li_2S_2) on the electrode's surface respectively [112]. Also, undesirable structural changes and pulverization can take place during cycling due to large volumetric changes. Moreover, during discharging, which is a multi-step process, sulfur can produce lithium polysulfide (LiPS) that is dissolvable in organic electrolytes. This can produce ''shuttle effect'' during cycling and can also form a thin layer of Li_2S on anode's surface leading to higher impedance and poor capacity

retention [113]. Number of strategies including separation modification [114], electrolyte configuration [115], anode protection and cathode improvements [116] have been implemented to deal with these shortcomings. Particularly, nanocarbons such as graphene, activated carbon, carbon nanotubes and carbon nitrides with sophisticated porous structures have been used. These can work as conductive framework to adsorb LiPS and encapsulate insulated sulfur to improve cyclic performance and reduce impedance. Since pure carbon framework is nonpolar and LiPS consists of polar molecules, this can result in limited trapping of LiPS molecules due to weak interactions between carbon and LiPS molecules. Therefore, graphitic-C_3N_4 can be a promising host material for sulfur with typical two dimensional layered structure similar to graphite with very high nitrogen content since recent studies have shown improved anchoring of LiPS through nitrogen doped polar carbon matrix [117]. In this section, we will discuss the use of graphitic-C_3N_4 in LISBs in detail.

As discussed earlier, graphitic-C_3N_4 can be a suitable sulfur host thanks to its excellent conductivity to offset the resistive nature of sulfur. Furthermore, stacked 2D sheets of nitrogen bridged triazines (C_3N_3) of graphitic-C_3N_4 can have strong interactions with LiPS by forming S_x-Li-N chemical bonds between Li atoms of Li_2S_n and undercoordinated N atoms of graphitic-C_3N_4 [118,119]. However, exceptionally high level of nitrogen content (up to 60%) can have adverse impact on the electrical conductivity of active material thereby resulting in poor electrochemical performance of LiSBs. A recent study by M Du and co-worker where they successfully synthesised graphitic-C_3N_4 with controlled nitrogen content between 2 and 60% using magnesiothermic denitriding technology and analysed its impact on electrochemical performance of LSB cell displayed promising results. Optimized nitrogen content of 6% with pore volume of 2 cm^3 and large specific surface area of 594 $m^2\ g^{-1}$ displayed superior electrochemical performance. This graphitic-C_3N_4 based sulfur host material delivered high specific capacity of 852.2 mA h g^{-1} at 0.5 C with a low-capacity decay of 0.12% per cycle after 300 cycles [120]. As discussed above, graphitic-C_3N_4 contained high nitrogen content including graphitic-N, pyrrolic-N, and pyridinic-N when compared with other carbon materials where nitrogen is introduced on the surface or within the material matrix. Nitrogen doped carbons in general and graphitic-C_3N_4 in particular involve in strong chemical interaction with polar LiPS especially due to the presence of pyridinic-N [121]. However, the layered structure of graphitic-C_3N_4 and very high nitrogen content can result in lower specific surface area and poor conductivity respectively. In a recent study, graphitic-C_3N_4 with porous tubular structure was produced to enhance its specific surface area in order to increase the number of electrochemically active sites. Also, this highly porous graphitic-C_3N_4 was doped with oxygen during synthesis stage using simple hydrothermal procedure to improve the electronic conductivity compared with bulk graphitic-C_3N_4. This oxygen doped graphitic carbon nitride (O-GCN) was used as cathode in LiSB which resulted in improved adsorption of lithium sulphides on the surface of O-GCN. This was mainly due to the strong electronegativity of surface of active materials originating form oxygen functional groups. Additionally, LiPS was also efficiently used because of the strong Li-O interactions. This oxygen rich cathode delivered high initial specific capacity of 1207 mA h g^{-1} with excellent capacity retention at 2C. Moreover, very low decay in long term capacity per cycle was observed after 1000 cycles. High capacitive performance was attributed to high surface area provided by tubular structure whereas good cyclability was credited to the reduced ‘‘shuttle effect’’ and excellent ionic movement offered by cathode’s tubular structure [122].

Impeded commercialisation of LSBs can largely be overcome by improving these three parameters of host material i.e., enhancing conductivity, polarity, and sulfur loading. Number of different strategies have been deployed to achieve this including the synthesising the graphitic-C_3N_4 hybrids since graphitic-C_3N_4 has inherently low sulfur loading and inferior conductivity. However, graphitic-C_3N_4 has unique two dimensional graphitic-phase structure, simple synthesis process, cost-effectiveness, rich with nitrogen functional groups and retains highly desirable physicochemical characteristics. Therefore, it can be anticipated that by combining graphitic-C_3N_4 with another suitable nanomaterials can make this hybrid an ideal candidate for superior electrochemical performance of LSBs. A three-dimensional conductive structure was constructed by combing graphitic-C_3N_4 and carbon nanotubes (CNTs) which is schematically displayed in Figure 5a. This was possible due to the possibility of the formation of strong hydrogen bonds with melamine of cyanuric acid molecules, yielding highly stable supramolecular structures [123]. Figure 5 also reveals other physical and electrochemical properties of graphitic-C_3N_4, CNTs and graphitic-C_3N_4 /CNTs composite. Figure 5b,c show typical characteristics peaks of CNTs and graphitic-C_3N_4 along with their respective SEM micrographs. SEM image in Figure 5b shows the tubular structure of CNTs whereas in Figure 5c SEM image shows sheet like structure of GCN. In Figure 5c two different but typical peaks of graphitic-C_3N_4 and CNTs can be observed from XRD patterns confirming the formation of pure hybrid without any contaminations. However, SEM micrographs in Figure 5c reveal a 3D structure formed by combing two-dimensional graphitic-C_3N_4 GCD and one-dimensional CNTs and this 3D structure can be highly conductivity and can provide with active sites as a sulfur host. XRD in (Figure 5d represents the presence of sulfur since sulfur was loaded using melting method also SEM micrographs appear very smooth due to the surface covering

with elemental sulfur. Figure 5e shows the charge—discharge profiles of the graphitic-C_3N_4 /CNTs/S cell at different rates where the charge discharge profile exhibits typical profiles with two discharge plateaus at approximately 2.4 and 2.1 V, these can be associated with the formation of soluble long-chain polysulfides. Figure 5f represents the Nyquist plots of the graphitic-C_3N_4 /CNTs/S where their solid electrolyte interface (SEI) layer and charge transfer resistances are low indicating good charge/electronic transfers. Figure 5g shows the reversible capacity where its initial reversible capacity is 1023.6 mAh g^{-1} and retains a capacity of 583.7 mAh g^{-1} after 500 cycles where the minimum drop per cycle is 0.08% [124]. This makes synthesis of hybrids using graphitic carbon nitride and other suitable nanomaterials using simple procedures an exceptionally useful strategy to address the technological deficiencies still remain in LiSBs to make these devices a market success. Furthermore, a recent study revealed that when graphitic-C_3N_4 is used to modify Li-metal surface it helped in uniform deposition of Li-ions which result in improved battery performance and reducing cell failures. Therefore, use of graphitic-C3N4 both as electrode and electrolyte additive can be highly beneficial to improve performance of devices [120].

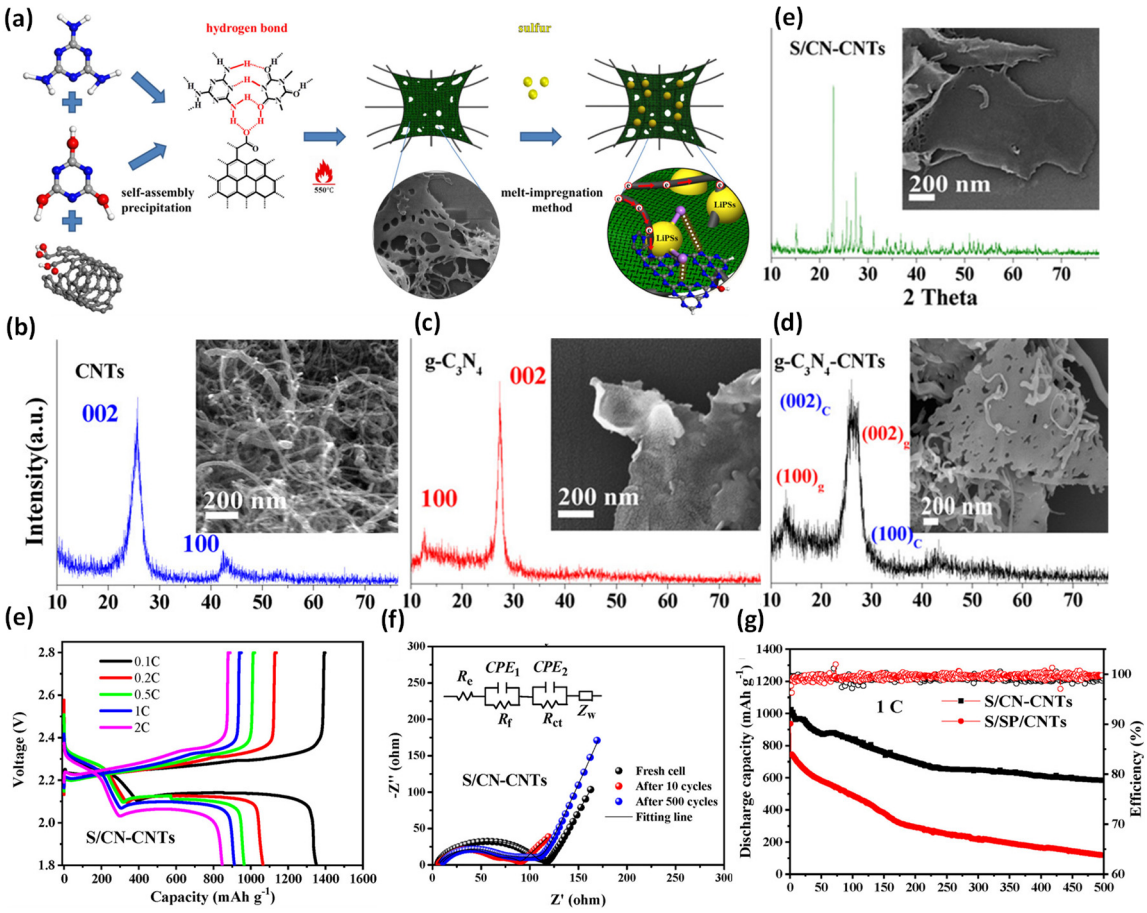

Figure 5. (**a**) Graphical illustration of graphitic-C_3N_4/CNTs composite synthesis, (**b**) XRD pattern/ SEM micrograph of CNTs, (**c**) XRD pattern/ SEM micrograph of graphitic-C_3N_4, (**d**) XRD pattern/ SEM micrograph of graphitic-C_3N_4/CNTs, (**e**) XRD pattern/ SEM micrograph of GCN/CNTs/S, (**e**) charge—discharge profiles of the graphitic-C_3N_4/CNTs/S cell at different rates, (**f**) the Nyquist plots of the graphitic-C_3N_4 /CNTs/S under different conditions and (**g**) reversible capacity of different samples [124].

Graphitic-C3N4 has been widely investigated as an active material in rechargeable battery systems and particularly in LSBs. Various performance characteristics extracted from recent literature have been presented in Table 1 when graphitic-C_3N_4 was adopted as electrode. Effect of electrode and electrolyte materials and variable operating parameters on the capacitive and cyclic performance has been included.

Table 1. Performance characteristics of graphitic-C_3N_4 and its composites when used as lithium host in LSBs.

Material	Specific Capacity (mA h g^{-1})	Capacity Retention (mAh g^{-1}—Cycles)	Electrolyte	Ref.
g-GCN@HPC	804.1 @ 1.0 C	757 after 250 cycles	1M LiTFSI + 0.2 M $LiNO_3$	[125]
GCN/rGO	752 @ 1.0 C	506 after 250 cycles	1M LiTFSI + 0.2 M $LiNO_3$	[126]
O-g-GCN-S	798 @ 1.0 C	465 after 1000 cycles	1M LiTFSI + 1% wt $LiNO_3$	[127]
N deficient g-GCN	734 @ 1.0 C	620 after 300 cycles	1M LiTFSI + 2% wt $LiNO_3$	[97]
PTCN/S	1156 @ 0.2 C	941 after 100 cycles	1M LiTFSI + 1% wt $LiNO_3$	[128]
S/GCN-CNTs	1351.2 @ 0.1 C	77.1% after 200 cycles	1M LiTFSI + 2% wt $LiNO_3$	[124]
g-C_3N_{4-x}/CNT	1128 @ 0.2 C	774 after 100 cycles	1M LiTFSI + 1% wt $LiNO_3$	[129]
O-TCN/S	704 @ 0.5 C	401 after 1000 cycles	1M LiTFSI + 0.25 M $LiNO_3$	[122]
GCN	852 @ 0.5 C	534 after 300 cycles	1M LiTFSI + 1% wt $LiNO_3$	[120]
GCN@rGO/S	1000.6 @ 0.1 C	87% after 200 cycles	1M LiTFSI + 1% wt $LiNO_3$	[130]

Graphitic Carbon Nitride (g-C_3N_4)—GCN.

Understanding of the underpinning chemistry of lithium-sulfur batteries and cell assembly techniques are maturing with time. Reports are being published recently suggesting that the LSBs may be close to industrial production however there are still certain shortcoming requiring dealing with such as inferior volumetric energy densities than LIBs [131]. Moreover, LSB cells are also still miniature size coin cells that are being used for laboratory testing and are operated under controlled laboratory conditions [132]. If successful, LSBs can have wide ranging applications including UAVs, heavy duty utility vehicles and large-scale energy storage systems due to low cost, light weight, and superior capacity.

4.2. Lithium-Ion Batteries (LIBs)

Over the past three decades, immense technological advancement has been made in Li-based battery systems, both in academia and industry. Capacity performance of LIBs is predominantly dependent on the type of electrolytes and electrode materials (anode/cathode) used. At present, commercially available LIBs traditionally use graphite as an electrode, the theoretical capacity of graphite is around 372 mA h g^{-1} which is considered to be the limiting factor in the capacitive performance of LIBs [133]. One of the major factor of using graphite instead of Li-metal, developed by Sony, is the lower cost and layered structure of graphite with optimised inter layer distance which can be advantageous for intercalation and de-intercalation of Li-ions especially at lower and moderate current densities [134]. However, it is imperative to improve the chemical and structural characteristics of these carbon-based electrodes in order to enhance the reversibility at higher current rates. It has been stated recently that the presence of heteroatoms such as nitrogen on the surface of carbon-based active materials can be highly beneficial due to the introduction of special functionalities. Graphitic-C_3N_4 which can be prepared by thermal treatment of various compounds such as urea and melamine which is inherently nitrogen rich, came to limelight and has been utilised in applications including water splitting and photocatalysis recently [43]. Graphitic-C_3N_4 can also be a potential active material for electrochemical energy storage and conversion applications in batteries/supercapacitors and fuel cells respectively where applications of Graphitic-C_3N_4 are less explored. Particularly for battery applications since Graphitic-C_3N_4 has similar structure as graphite with nearly identical inter layer spacing. Excellent chemical and exceptional thermal stability, desirable electronic properties are additional advantageous aspect for the selection of Graphitic-C_3N_4 for battery applications. It has been proposed that C and N connectivity in Graphitic-C_3N_4 forms interconnecting molecular islands of melem units on the 2D graphite like sheets leaving triangular gaps in between these triangular melem units to produce triangular void (pore) which can accommodate both charged and uncharged species [135]. Above mentioned properties make Graphitic-C_3N_4 a fascinating material to be investigated for its applications in LiBs which will be discussed in detail in this section.

Nitrogen doped carbons such as graphitic carbon nitride can be used as host material in rechargeable battery systems for superior energy and power performance. However, in case of Graphitic-C_3N_4 very high level of nitrogen content of up to 60% (57.1 atom % precisely) can have a negative effect on the performance of LIBs. Three types of nitrogen species are identified in its structure including pyridinic-nitrogen, graphitic nitrogen, and bridge-nitrogen. It was speculated in a theoretical study by Veith et al., that graphitic nitrogen from Graphitic-C_3N_4 tend to react irreversibly with lithium ions resulting in creation of structural disorder within Graphitic-C_3N_4. Therefore, reduction of nitrogen content can be suitable strategy to enhance the battery performance particularly to address the enormous capacity losses in case of LIBs [136]. During a research study, nitrogen deficient graphitic carbon nitride (ND- Graphitic-C_3N_4) was synthesised using magnesiothermic denitriding technology followed by

using it as an electrode in lithium-ion battery. The average capacity of 860 mA h g^{-1} at current density of 0.1 Ag^{-1} was achieved and ND- Graphitic-C_3N_4 samples retained high capacity of 328 mA h g^{-1} even at very high current density of 20 Ag^{-1} with capacity going back to 1121 mA h g^{-1} immediately when the current density was dropped down to 0.1 Ag^{-1}, exhibiting excellent reversibility. Highest capacity 2753 mA h g^{-1} at current density of 0.1 Ag^{-1} attained for ND- Graphitic-C_3N_4 sample on 190th cycles which was much higher than 61 mA h g^{-1} after 100th cycles, for original Graphitic-C_3N_4 sample [96]. Nitrogen doped amorphous carbons can also be used as electrode for enhanced performance rechargeable batteries. One of the major reason behind the selection of amorphous nanocarbons is to overcome the limitation of theoretical limit (372 mA h g^{-1}) of graphite anode. Numerous strategies have been developed to prepare nitrogen doped amorphous carbons. Zhang, Wenli, et al., in a recent study, produced nitrogen doped carbon from graphitic carbon nitride. Zinc-assisted thermal treatment of Graphitic-C_3N_4 enabled them the carbonization of graphitic carbon nitride which resulted in successful synthesis of nitrogen-doped carbon with nitrogen content of 21.6 atom%. Graphitic carbon nitride derived from nitrogen doped carbon (ND- Graphitic-C_3N_4) displayed capacity of 686 mA h g^{-1} at current density of 50 mAg^{-1}. Although ND- Graphitic-C_3N_4 experienced a decreased capacity in the first few cycles however it displayed a very stable cycling performance during the following 2500 cycles with a stable capacity of 323 mA h g^{-1}. Figure 6 shows various physical, chemical, and electrochemical characteristics of ND- Graphitic-C_3N_4 sample. Figure 6a–c shows the SEM images of ND- Graphitic-C_3N_4 sample, Figure 6a displays the non-amorphous structure of ND- Graphitic-C_3N_4 whereas (b) shows the thickness of ND- Graphitic-C_3N_4 sheets which are in nanometres and finally Figure 6c confirms the layered structure of ND- Graphitic-C_3N_4. Figure 6d,e shows C 1s and N 1s high-resolution XPS spectra of ND- Graphitic-C_3N_4 sample. Spectra in Figure 6d confirms the successful incorporation of heteroatoms of nitrogen since the presence of CAC (284.4 eV), C@N (285.6 eV), and CAN (286.7 eV) bonds, and minor CAO bonds. These bonds are the indication of nitrogen functional groups where it specifies the N doping configurations which are mainly pyrrolic nitrogen (N-5) (399.5 eV) (52.05%), and pyridinic nitrogen (N-6) (398.0 eV) (43.35%) with only a small portion of graphitic nitrogen (NAQ) (4.6%). Figure 6f represents the XRD spectra of ND-Graphitic-C_3N_4 where final product contains zinc cyanamide and unreacted zinc metal however the intensity of ND-Graphitic-C_3N_4 is too weak to be detected. CVs curves recorded at different scan rates are shown in Figure 6g demonstrating the excellent rate capability of ND- Graphitic-C_3N_4 anode. More importantly, impedance reduces with cycling of ND- Graphitic-C_3N_4 electrode as can be seen from Figure 6h since size of semicircle reduces with an increase in number of cycles. Finally, outstanding cyclic stability with Coulombic efficiency of more than 98.6% was also achieved [137].

Graphene can be another potential electrode material to substitute graphite in order to enhance capacitive performance beyond 372 mA h g^{-1}. However, complicated synthesis procedures and low yields are some of the key challenges for the adoption of graphene in rechargeable batteries [138]. Furthermore, heteroatoms doping is found to be highly effective for performance enhancement of batteries. Graphitic-C_3N_4 can assist in overcoming these challenges since it has a two-dimensional layered structure similar to that of graphene and is inherently rich with nitrogen functional groups coupled with ease of synthesis (single step thermal process) which can help in achieving scalability. Transition metal oxides (TMOs) have also been widely investigated as electrode for LIBs because of their superior lithium storage capacity. However, TMOs are not used as electrode in their pure form due to their poor electronic conductivities, volume expansions, agglomeration, and particle pulverization during cycling [139]. Therefore, synthesis of Graphitic-C_3N_4/TMOs composites for LIBs seems a suitable strategy to improve LIBs performance. $ZnFe_2O_4$/Graphitic-C_3N_4 was prepared and investigated for its suitability as anode in LIBs by Joshi, Bhavana, and co-workers. The selection of $ZnFe_2O_4$ was made since mixed transition metal oxides (MTMOs) are highly desirable in rechargeable battery applications due to their superior electrochemical performance thanks to their different working potentials. During this study Graphitic-C_3N_4/TMOs composite anodes achieved initial reversible capacities of 1550 mA h g^{-1} at 50 mA g^{-1} and up to 934 mA h g^{-1} at 1000 mA g^{-1} after 20 cycles. The superior electrochemical performance and capacity retention (88% after 160 cycles at 100 mA g^{-1}) are attributed to highly reversible alloying/conversion mechanisms. This study provided proof of concept for the utilisation of low cost and abundant earth metals in conjunction with Graphitic-C_3N_4 [140]. Table 2 provide overview of different performance indicators when different electrodes based on Graphitic-C_3N_4, and its composites are used in LIBs.

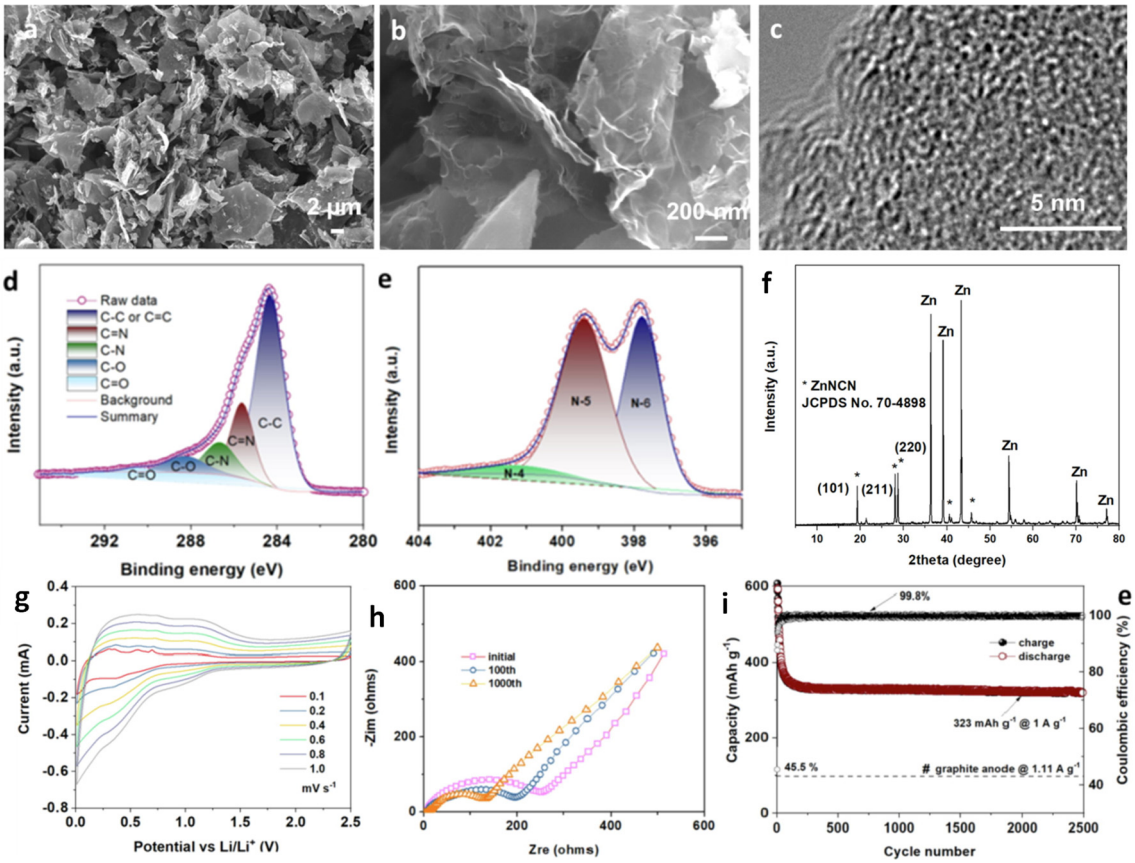

Figure 6. (**a**,**b**) SEM images of ND-GCN nano-sheets (**c**) HRTEM image of ND-Graphitic-C_3N_4, (**d**) C 1s, (**e**) N 1s high-resolution XPS spectra of ND-Graphitic-C_3N_4 sample (**f**) XRD spectra (**g**) CV curves at different scan rates (**h**) Nyquist plots after different GCD cycles and (**i**) Long-term cycling stability of ND- Graphitic-C_3N_4 at a current density of 1 A g^{-1} [137]. * Diffraction patterns for reference from JCPds database for ZnNCN structure.

Table 2. Performance characteristics of Graphitic-C_3N_4 and its composites when used in LIBs.

Material	Specific Capacity (mA h g^{-1})	Capacity Retention (mAh g^{-1}—Cycles)	Electrolyte	Ref.
huCP/g-C_3N_4	1030 @ 1Ag^{-1}	360 after 4000 cycles	1 M LiPF6 (ED/DMC)	[141]
CNNC	686 @ 50 mAhg^{-1}	323 after 2500 cycles	1 M $LiPF_6$ (ED/DMC)	[137]
GCN/rGO	1632 @ 50 mAhg^{-1}	970 after 300 cycles	1 M $LiPF_6$ (EC/DEC)	[142]
Ni-g-C_3N_4	678.3 @ 50 mAhg^{-1}	487.1 after 600 cycles	1 M $LiPF_6$ (EC/DEC)	[143]
ZFCN	1550 @ 50 mAh g^{-1}	1235 after 160 cycles	1 M $LiPF_6$ (EC/DEC)	[140]
ND-g-C_3N_4	2627 @ 0.2 A g^{-1}	2753 after 300 cycles	1 M $LiPF_6$ (EC/DEC)	[96]
g-C_3N_4	140	54 after 40 cycles		[39]
CuS/g-C_3N_4	304 @ 0.1 A g^{-1}	478.4 after 100 cycles	1 M $LiPF_6$ (EC/DMC)	[144]

4.3. Sodium-Ion Batteries (NIBs)

LIBs have dominated the rechargeable battery market for more than thirty years thanks to their advantageous characteristics including long cycle life, high energy density, and good rate capability when compared to other RBs. Further technological advancement and commercialisation of LIBs can reduce our reliance on fossil fuels however it can result in short supply of lithium due to limited lithium resources and uneven geographical distribution of lithium reserves [145]. Therefore, it is vital to find an alternative technology to substitute LIBs which has merits including cost-effectiveness, natural abundance and environmentally friendliness with battery chemistry and performance similar to that of lithium-ion battery. NIBs batteries have been investigated vigorously as a likely replacement of LIBs due to low cost, wider availability (23,600 ppm in the earth crust), and similar battery chemistry. Furthermore, Na has an ideal redox potential of −2.7 V against the standard hydrogen electrode (SHE) than that of Li^+ (−3.04 V versus SHE) [146]. Also, it shows smaller Stroker's radius because of its weaker Lewis acidity which lowers activation energy of ion diffusion resulting in better ionic diffusion of electrolyte [147]. Another advantage of NIBs is the use of more cost-effective Al based current collectors instead of costly Cu based current collector used in LIBs due to the inertness of Na^+ ions towards Al. Performance of NIBs has improved greatly

over the years with the improvements in its technology however sluggish reaction kinetics due to slow ionic migration still an immense challenge because of the larger ion size of Na^+ (1.02 Å) compared with Li^+ (0.76 Å), resulting in huge irreversible capacity losses during cycling [148–150]. Therefore, the development of well-ordered porous electrode in a cost effective and environmentally friendly manner which can address this issue is still an enormous challenge. Recently, Graphitic-C_3N_4 has seen increased applications in electrochemical energy storage and conversion systems that is due to its typical porous structure consists of stacked one-atom-thick planar sheets of sp2 hybridized carbon coupled with the nitrogen atoms exhibiting distinctive physicochemical and electrochemical characteristics [38,151–153]. Nitrogen functionalised graphitic-C_3N_4 where nitrogen can be highly beneficial as it can enhance the Na^+ ionic uptake due to higher electronegativity than carbon. Nevertheless, further functionalisation with sulfur can also be a suitable strategy to boost NIBs performance, since sulfur has larger ionic radius of (S: 102 pm) than nitrogen and carbon (N: 75 and C: 77 pm) which can assist in extending the interlayer spacing of graphitic-C_3N_4 frameworks leading to improve interaction-de-intercalation of Na^+ ions [141,154]. A study by Cha, Wangsoo, et al., where order mesoporous structure of graphitic-C_3N_4 was produced coupled with sulfur doping which resulted in capacitive performance comparable to those of LIBs, schematic of synthesis strategy is shown in Figure 7a. Figure 7b,c display the interlayer scaping and graphical presentation of intercalation and de-interaction of Na^+ ion within sulfur doped graphitic-C_3N_4 respectively. All the graphitic-C_3N_4 samples displayed high specific surface area, and this increased with increasing carbonisation temperature which can be attributable to the release of sulfur and nitrogen from the material matrix at elevated temperature resulting in introducing microporosity. The Brunauer–Emmett–Teller (BET) isotherms are shown in Figure 7d which exhibit a type IV isotherm with a hysteresis loop which indicates the presence of well-ordered cylindrical mesopores. The positive impact of nitrogen and sulfur doping into carbon is experimentally proved through electrochemical measurement when this double doped material is used as an anode for SIB. Figure 7e shows the 1st and 2nd CV cycles displaying a significant loss around 0.6V which can be due to the SEI (solid electrolyte interface) layer formation due to the decomposition of electrolyte. Figure 7f displays the EIS spectra, it can be witnessed that sulfur and nitrogen doped samples has the smallest semicircle in high frequency region displaying the highest electrical conductivity. The ratio of capacitive contribution rises with increasing the scan rate and finally reaches to 93.8% at a scan rate of 1 mV s^{-1} as shown in Figure 7g. Co-doped samples have lower Columbic efficiency in first cycle which can be credited to the high specific surface as discussed earlier and has been shown in Figure 7h [155].

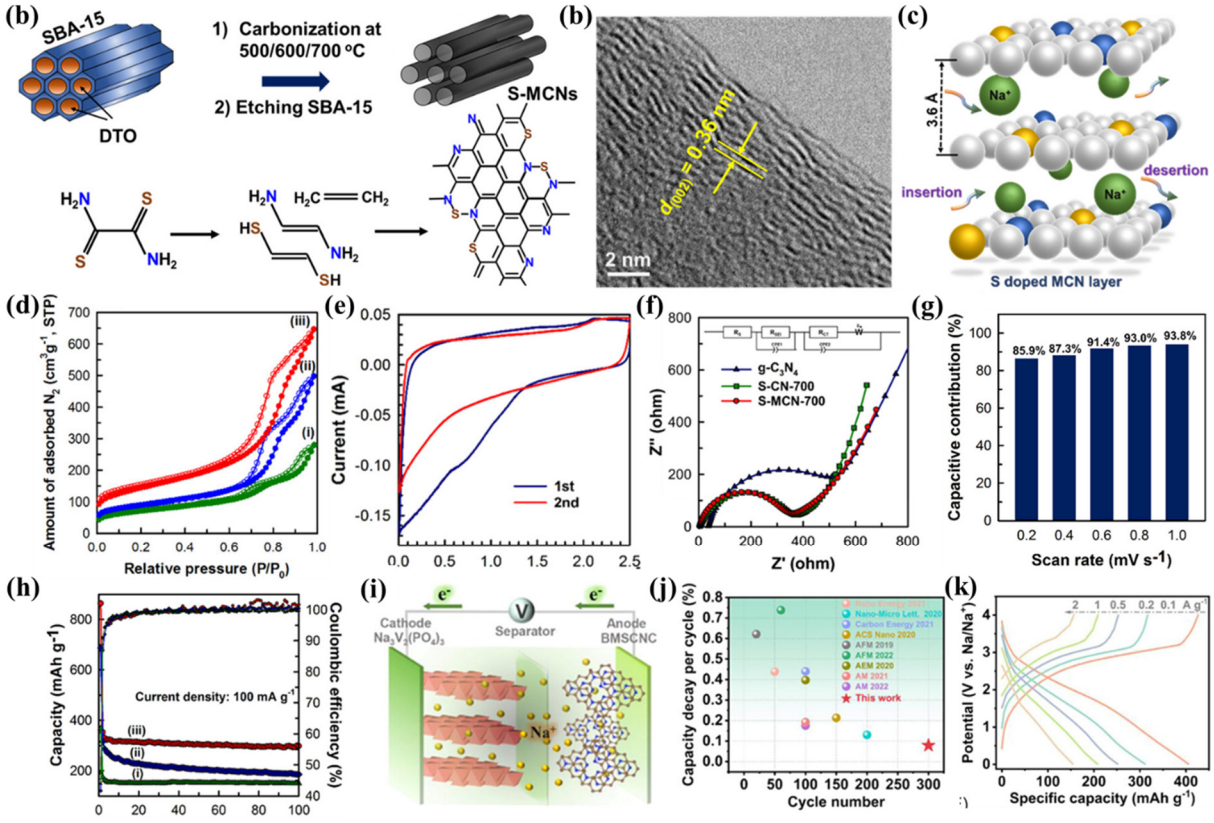

Figure 7. (**a**) schematics presentation of the synthetic procedure of nitrogen and sulfur co-doped graphitic-C_3N_4, (**b**) interlayer spacing using HR-TEM image of graphitic-C_3N_4 sample, (**c**) graphical representation of

intercalation/de-intercalation of sulfur doped graphitic-C_3N_4 electrodes, (**d**) BET adsorption/desorption isotherms, (**e**) CV curve of dual doped sample at a scan rate of 0.2 mV s^{-1}, (**f**) Nyquist plots over the frequency range between 100 kHz and 0.01 Hz of different doped/un-doped samples, (**g**) capacity retention comparison at different scan rates, (**h**) cycling performances with a Columbic efficiency [155,156].

The application of graphitic-C_3N_4 in wider battery applications still limited due to it lower crystallinity and unknown impact of nitrogen component especially pyrrolic-N functional groups. A recent was conducted to fine-tune nitrogen content and critical role of pyrrolic-N for enhancing charge transfer and enhancing Na^+ storage in graphitic-C_3N_4 based composites. A schematic of the full cell is shown in Figure 7i whereas Figure 7j,k GCD profiles and capacity decay comparison with previous studies respectively. It can be seen the outstanding charge-discharge performance and capacity retention of these hybrids [156]. Table 3 displays various performance traits of different electrodes based on graphitic-C_3N_4 in conjunction with various electrolytes.

Table 3. Performance characteristics of graphitic-C_3N_4 and its composites as an electrode in NIBs.

Material	Specific Capacity (mAh g^{-1})	Capacity Retention (mAh g^{-1}—Cycles)	Electrolyte	Ref.
MoS_2-ND-C_3N_4	610.66 @ 0.1 A g^{-1}	365.8 after 500 cycles	1 M $NaClO_4$	[157]
Sn/D-C_3N_4	518.3 @ 1.0 A g^{-1}	436.1 after 500 cycles	1 M $NaFP_6$	[158]
huCP/g-C_3N_4	1030 @ 1.0 A g^{-1}	360 after 4000 cycles	1 M $NaPF_6$	[141]
3D-ENTC	420 @ 50 mA g^{-1}	243 after 500 cycles	1 M $NaPF_6$	[159]
g-C_3N_4@RGO	170 @ 0.1 A g^{-1}	146 after 2000 cycles	NaFSI	[160]
S-MCN	304.2 @ 100 mA g^{-1}	64 after 1000 cycles	1 M $NaClO_4$	[155]
C/g-C_3N_4	254 @ 0.1 A g^{-1}	120 after 14000 cycles		[161]
C_{60}@GCN	430.5 @ 0.05 A g^{-1}	101.2 after 5000 cycles		[37]
Fe_2O_3/GCN	660.3 @ 0.1 A g^{-1}	159.9 after 300 cycles	1.0 M $NaClO_4$	[162]
EGrO	268@100 mAg^{-1}	60.84% after 2000 cycles	1 M $NaClO_4$-PC	[158]

As discussed in detail in this section, key benefit of two-dimensional materials such as graphitic-C_3N_4 is that it can extend battery life since it has fewer layers with wider interlayer spacing which can reduce volumetric changes caused by insertion/extraction of metal ions during cycling. Although graphitic-C_3N_4 nanosheets has inferior conductivity when compared with graphene due to high nitrogen content however reduced nitrogen has resulted in improved conductivity. Furthermore, composites of graphitic-C_3N_4 with other nanomaterials including graphene, carbon nanotubes and transition metal oxides has resulted in not only improved conductivities but also enhanced capacities which can potentially broaden electrochemical battery applications of graphitic-C_3N_4.

4.4. Graphitic-C_3N_4 as Electrode for Metal Air Batteries (MABs)

MABs have an immense potential to become a sort after energy storage device for large number of commercial applications in near future these applications can include transportation and portable consumer electronic thanks to their excellent power to weight ratios and much superior theoretical capacities. Unlike LIBs, wider availability of raw material at lower costs, huge potential of recycle-ability and lower level of toxicity make these devices highly desirable [103,163,164]. However, at current stage, commercial scale distribution has been constrained due to the inferior rate capabilities of the cathode catalyst for oxygen electrode reactions which involves multiple electron-proton transfers at a triple phase interface (solid catalyst, liquid electrolyte, gaseous oxygen). Typically, a complete OER/ORR in an appropriate electrolyte using an ideal catalyst, follows a $4e^-$ transfer process [165,166]. Due to larger energy barrier for O_2 formation/dissociation on most catalysts, the reaction is impeded because of the invariably leading to alternate pathways which can generate stable intermediates that block active sites [151]. This requires the exploration and selection of suitable alternative catalysts which retain attributes such as superior electronic conductivity, durability and lower O_2 formation/dissociation energy barrier. Ru, Pt and Ir are the most commonly adopted catalysts however, the rarity of these materials results in elevating the production cost [167–170]. Therefore, research for highly stable and cost-effective catalyst which can compete equally in terms of OER/ORR performance to those of widely adopted precious metals is of paramount importance.

Graphitic-C_3N_4, among other non-metal electrocatalysts have gain much attention recently due to it cost-effective and environmentally friendly production coupled with excellent chemical stability and electrical conductivity while maintaining $4e^-$ oxygen activity [170]. What sets graphitic-C_3N_4 apart from conventional carbo-nitro compounds is their polymeric nature, thermo-chemical stability, high surface area and most important of all,

electron-rich properties owing to the presence of N lone-pair electrons, rendering them, as sites for metal inclusion and electronic modification of molecular structures. Graphitic-C_3N_4 can be employed in number of different functionalities as is shown in a recent studies where transition metal oxide (TMO) and metal organic frameworks (MOFs) were combined to produce a catalyst. However, to integrate TMO and MOF required appropriate substrate which not only avoid the agglomeration but can also enhance the porous structure at elevated temperature. A non-precious and cost-effective bifunctional oxygen catalyst Co_3O_4 encapsulated within nitrogen defect-rich graphitic-C_3N_4 was synthesised by graphitizing the zeolitic imidazolate framework (ZIF)-67@ND-CN as shown schematically in Figure 8. Hierarchical and highly porous layered structure full of defects of graphitic-C_3N_4 was constructed as shown in Figure 8a where this excellent porosity could be attributed to destruction of the ring structure of the 3-s-triazine. Layer thickness increased substantially as displayed in Figure 8b which can be credited to the unique architect of zeolitic imidazolate framework (ND-CN) where no agglomeration took place at elevated temperature. Co_3O_4@ND-CN hybrid was produced through heat treatment at 350 °C where the deposition of Co_3O_4 particles on wrinkled ND-CN sheets is visible from Figure 8c. This produced material resulted in much higher level of porosity and abundant pore structure which can witnessed from the adsorption/desorption isotherms displayed in Figure 8d whereas the inset displays the pore size distribution. High specific surface 365.67 m^2g^{-1} which can be corelated to higher nitrogen intake and average distribution stayed with the range of 5–240 nm which can be beneficial for the transportation of protons and ions within the structure of the material. ORR activity of catalyst was investigated in an alkaline electrolyte using cyclic voltammetry at 20mVs^{-1}. A distinct oxygen reduction peak at 0.8 V was visible as shown in Figure 8e implying the potential high activities of Co_3O_4@ND-CN for ORR whereas Figure 8f exhibits comparison between the half-wave potential and overpotential of catalysts.

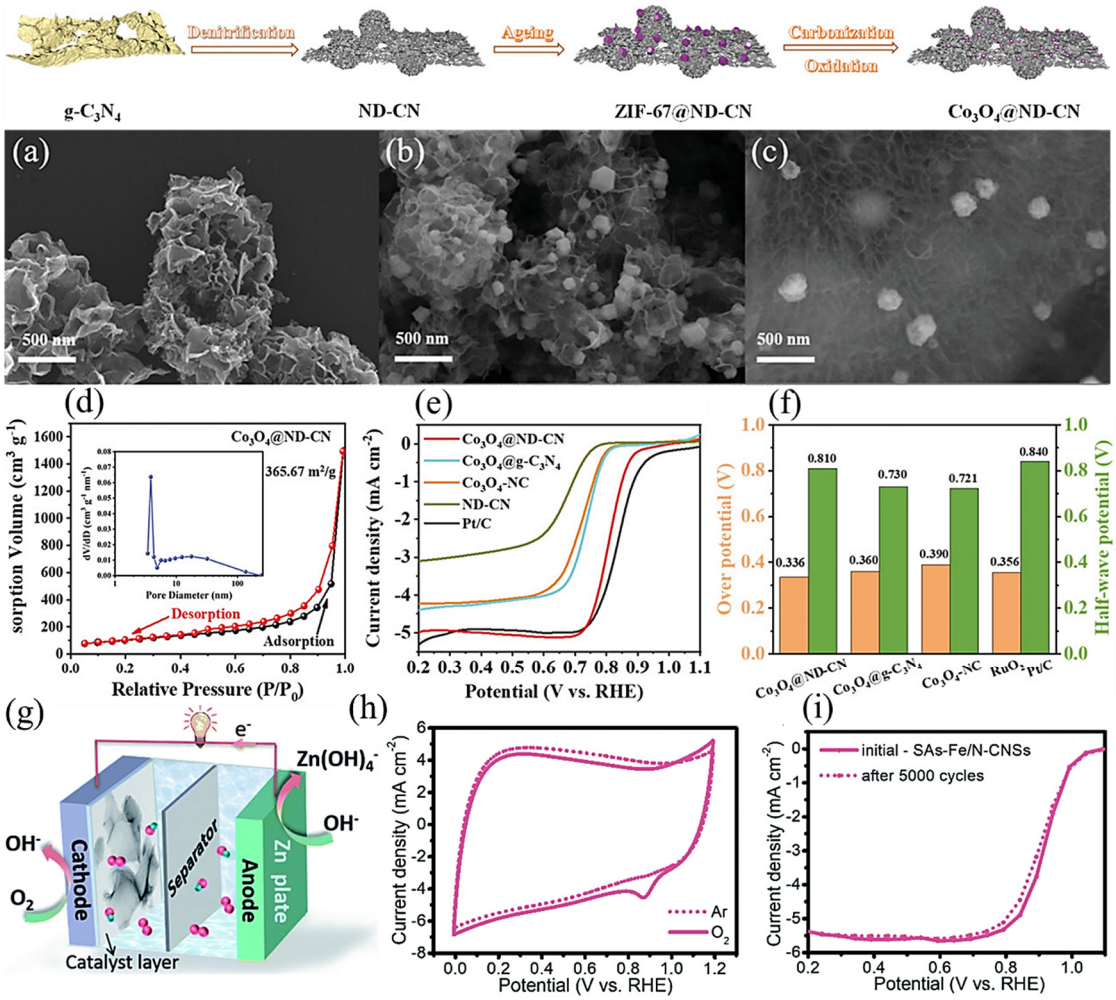

Figure 8. schematic illustration of Co_3O_4-ND-CN hybrid, SEM micrographs of (**a**) ND-CN, (**b**) ZIF-67@ND-CN, (**c**) Co_3O_4@ND-CN, (**d**) nitrogen adsorption-desorption isotherms and pore size distribution (inset) of Co3O4@ND-CN, (**e**) LSV curves of the ORR in an O_2-saturated 0.1 molar KOH solution at 10 mV s^{-1}, (**f**) Comparison between the half-wave potential and overpotential of catalysts, (**g**) schematic presentation of a typical primary Zn–air battery, (**h**) cyclic voltammetry profile within Ar-/O_2-saturated 0.1 M KOH and (**i**) SCV profile of samples before and after 5000 cycles [171,172].

Graphitic-C_3N_4 can also be used as structure guiding two-dimensional template to produce variety of catalysts. In a study by Gong, Xiao-Fei, et al., where they produce Fe–Nx center-embedded N-doped carbon nanosheets and used these materials for catalyst for Zinc-air battery and schematic of that battery systems is shown in Figure 8g. To assess ORR activity cyclic voltammetry measurement were carried out in 0.1 molar KOH where distinctive peak ORR cathode peak is present around 0.87 V as shown in Figure 8h. The produced catalyst displayed excellent stability with capacity retention of over 92% well exceedingly commercially available very expensive catalyst based on Pt/C with retention of around 78% as displayed in Figure 8i. The fantastic electrochemical performance of Zn–air batteries with a maximum power density of 157.03 mW cm^{-2} signifies promising application of material derived using graphitic-C_3N_4 in practical applications related to electrochemical energy storage. Commercialisation of metal air batteries based graphitic-C_3N_4 catalyst can prove a significant improvement making these devices a resounding success since studies have already proved that graphitic-C3N4 catalyst can outperform commercially available catalysts such as Pt/C based catalysts [151,173]. Table 4 below discusses number of electrochemical performance parameter of MABs when graphitic-C_3N_4, its derivatives and composites are used as catalyst.

Table 4. Performance characteristics of graphitic-C_3N_4 and its composites when used in MABs.

Material	Specific Capacity (mA h g^{-1})	Capacity Retention (mAh g^{-1}—Cycles)	Electrolyte	Ref.
P,S-CNS	970 @5 mA cm^{-2}	830 after 500 cycles	6 M KOH	[174]
$CoSe_2$@g-C_3N_4	2158 @ 0.1 mA cm^{-2}		0.5 M $LiClO_4$	[175]
PS-CNFs	698 @ 20 mA cm^{-2}	120 hours	0.1M KOH	[176]
GF (g-C_3N_4/GF)	390 @ 0.2C	280 after 400 cycles	2 M $ZnSO_4$	[177]
CoSA/NCs	908.7 @ 20 mA cm^{-2}		0.1 M KOH	[178]
NG	352 @0.2 mA/cm^{-2}	324 after 30 cycles		[175]

5. Conclusions and Future Outlook

In this review, succinct introduction of graphitic-C_3N_4 which retains a layered structure while retaining distinct characteristics regarding both material and performance has been presented within the early part of this article. This is followed by concise discussions around frequently used state-of-the-art synthesis strategies such as supramolecular self-assembly, templating, sol-gel, and exfoliation methods to produce graphitic-C_3N_4. Finally, we have devolved into detailed discussion of the applications of graphitic-C_3N_4, its derivatives and composites in advanced battery systems consisting of lithium-ion, sodium-ion, lithium-sulfur and metal-air batteries. This study suggests that graphitic-C_3N_4 possesses an immense potential and can be a promising candidate to be an electrode active material in advanced/futuristic battery systems. The number of avenues can be explored for the enhanced utilisation of graphitic-C_3N_4 in advanced electrochemical energy storage in RBs where particular emphasis should be directed towards number of key areas including:

(i) Research has advanced from macro to nano scale; it will be highly beneficial to explore and optimize the electrode//electrolyte interface at nanoscale of these electrochemical energy storage systems when graphitic-C_3N_4 is used as an active material. Enhanced understanding gained through these studies will be vital in optimizing the cell designs and performance of these advanced rechargeable batteries particularly interfacial side reactions with metallic lithium/sodium which can lead to further innovation and commercialization in this area.

(ii) Fine-tuned synthesis of two dimensional graphitic-C_3N_4 with controlled surface chemistry, precise number of layers, size and interlayer spacing remains the area to be explored further. Since, the optimization of these parameters can result in maximizing the performance of these advanced battery systems.

(iii) Linking and fine-tuning the physicochemical properties of graphitic-C_3N_4 nanosheets with their electrochemical output is of paramount importance for the electrode design which can be brought into full and more targeted manner to improve performance e.g., graphitic-C_3N_4 can be functionalised easily using various functional groups to optimize its surface chemistry couple with high level of porosity enhancing adsorption characteristics e.g., for lithium polysulfides in case of LSBs.

(iv) Graphitic-C_3N_4 has started witnessing its applications in rechargeable batteries, however, it synthesis at commercial scale in cost effective manner with desired properties is still a challenge and requires further research.

In conclusion, by exploring these areas of research while adopting a holistic approach encompassing theoretical insights and experimental validations, we can unlock the full potential of graphitic-C_3N_4, its derivatives and composites for advanced and futuristic electrochemical energy storage.

Author Contributions

Q.A.: Writing original draft—review & editing, Conceptualization, Visualization, Methodology, Software. P.A.S.: Writing original draft—review & editing, Conceptualization, Visualization & Methodology. M.A.A.: Writing—review & editing, Supervision, Methodology, R.R.: Writing—original draft, Conceptualization, Visualization & Software. A.G.O.: Writing—review & editing, Validation, Resources, Supervision. All authors have read and agreed to the published version of the manuscript.

Funding

This research received no external funding.

Conflicts of Interest

The authors declare no conflict of interest.

References

1. Olabi, A.G.; Abbas, Q.; Shinde, P.A.; et al. Rechargeable batteries: Technological advancement, challenges, current and emerging applications. *Energy* **2023**, *266*, 126408.
2. Sarmah, S.; Lakhanlal; Kakati, B.K.; et al. Recent advancement in rechargeable battery technologies. *Wiley Interdiscip. Rev. Energy Environ.* **2023**, *12*, e461.
3. Abbas, Q.; Mirzaeian, M.; Hunt, M.R.; et al. Current state and future prospects for electrochemical energy storage and conversion systems. *Energies* **2020**, *13*, 5847.
4. Abbas, Q.; Khurshid, H.; Yoosuf, R.; et al. Engineering of nickel, cobalt oxides and nickel/cobalt binary oxides by electrodeposition and application as binder free electrodes in supercapacitors. *Sci. Rep.* **2023**, *13*, 15654.
5. Mu, T.; Wang, Z.; Yao, N.; et al. Technological penetration and carbon-neutral evaluation of rechargeable battery systems for large-scale energy storage. *J. Energy Storage* **2023**, *69*, 107917.
6. Patel, M.; Mishra, K.; Banerjee, R.; et al. Fundamentals, recent developments and prospects of lithium and non-lithium electrochemical rechargeable battery systems. *J. Energy Chem.* **2023**, *81*, 221–259.
7. Khan, T.; Garg, A.K.; Gupta, A.; et al. Comprehensive review on latest advances on rechargeable batteries. *J. Energy Storage* **2023**, *57*, 106204.
8. Singh, A.N.; Islam, M.; Meena, A.; et al. Unleashing the potential of sodium-ion batteries: Current state and future directions for sustainable energy storage. *Adv. Funct. Mater.* **2023**, *33*, 2304617.
9. Yu, T.; Li, G.; Duan, Y.; et al. The research and industrialization progress and prospects of sodium ion battery. *J. Alloys Compd.* **2023**, *958*, 170486.
10. Abu, S.M.; Hannan, M.; Lipu, M.H.; et al. State of the art of lithium-ion battery material potentials: An analytical evaluations, issues and future research directions. *J. Clean. Prod.* **2023**, *394*, 136246.
11. Song, Z.; Ma, Y.; Cheng, X.; et al. Development of advanced anodes for solid-state lithium batteries. *Mater. Today* **2025**, *88*, 1005–1027.
12. Huang, M.; Wang, X.; Liu, X.; et al. Fast ionic storage in aqueous rechargeable batteries: From fundamentals to applications. *Adv. Mater.* **2022**, *34*, 2105611.
13. Ma, H.; Wang, F.; Shen, M.; et al. Advances of $LiCoO_2$ in Cathode of Aqueous Lithium-Ion Batteries. *Small Methods* **2024**, *8*, 2300820.
14. Xin, Y.-M.; Xu, H.-Y.; Ruan, J.-H.; et al. A Review on Application of $LiFePO_4$ based composites as electrode materials for Lithium Ion Batteries. *Int. J. Electrochem. Sci.* **2021**, *16*, 210655.
15. Guan, J.; Liu, M. Transport properties of $LiMn_2O_4$ electrode materials for lithium-ion batteries. *Solid State Ion.* **1998**, *110*, 21–28.
16. Guo, F.; Hu, Z.; Xie, Y.; et al. Nanostructured $LiNi_{0.8}Co_{0.1}Mn_{0.1}O_2$ with a Hollow Morphology Boosting Cycling Stability as Cathode Materials for Lithium-Ion Batteries. *ACS Appl. Nano Mater.* **2024**, *7*, 15215–15222.
17. Ma, L.; Liu, G.; Wang, Y.; et al. Preparation and Performance of Regenerated Al2O3-Coated Cathode Material $LiNi_{0.8}Co_{0.15}Al_{0.05}O_2$ from Spent Power Lithium-Ion Batteries. *Molecules* **2023**, *28*, 5165.
18. Zhao, W.; Zhao, C.; Wu, H.; et al. Progress, challenge and perspective of graphite-based anode materials for lithium batteries: A review. *J. Energy Storage* **2024**, *81*, 110409.
19. Iqbal, M.Z.; Zakar, S.; Khizar, A.; et al. Investigating the potential of transition metal sulfides as electrode material for energy storage applications. *Appl. Phys. A* **2024**, *130*, 541.
20. Muthu, P.; Rajagopal, S.; Saju, D.; et al. Review of Transition Metal Chalcogenides and Halides as Electrode Materials for Thermal Batteries and Secondary Energy Storage Systems. *ACS Omega* **2024**, *9*, 7357–7374.

21. AbdelHamid, A.A.; Mendoza-Garcia, A.; Lee, S.S.; et al. Metal oxide-and metal-loaded mesoporous carbon for practical high-performance Li-ion battery anodes. *Nano Energy* **2024**, *119*, 109025.
22. Sun, Y.; Wu, Q.; Liang, X.; et al. Recent developments in carbon-based materials as high-rate anode for sodium ion batteries. *Mater. Chem. Front.* **2021**, *5*, 4089–4106.
23. Zhai, H.; Xia, B.Y.; Park, H.S. Ti-based electrode materials for electrochemical sodium ion storage and removal. *J. Mater. Chem. A* **2019**, *7*, 22163–22188.
24. Lee, M.; Kim, M.-S.; Oh, J.-M.; et al. Hybridization of layered titanium oxides and covalent organic nanosheets into hollow spheres for high-performance sodium-ion batteries with boosted electrical/ionic conductivity and ultralong cycle life. *ACS Nano* **2023**, *17*, 3019–3036.
25. Fang, Y.; Luan, D.; Lou, X.W. Recent advances on mixed metal sulfides for advanced sodium-ion batteries. *Adv. Mater.* **2020**, *32*, 2002976.
26. Gong, Y.; Li, Y.; Li, Y.; et al. Metal selenides anode materials for sodium ion batteries: Synthesis, modification, and application. *Small* **2023**, *19*, 2206194.
27. Park, J.; Han, D.; Son, J.P.; et al. Extending the Electrochemical Window of Na^+ Halide Nanocomposite Solid Electrolytes for 5 V-Class All-Solid-State Na-Ion Batteries. *ACS Energy Lett.* **2024**, *9*, 2222–2230.
28. Gupta, Y.; Siwatch, P.; Karwasra, R.; et al. Transition metal oxides as the electrode material for sodium-ion capacitors. *Nanofabrication* **2023**, *8*, 1–16.
29. He, L.; Guo, J.; Liu, S.; et al. Progress of metal phosphides as the anode materials for sodium ion batteries. *J. Alloys Compd.* **2024**, *997*, 174924.
30. Madhuri, A.; Jena, S.; Swain, B.P. Transition Metal Nitrides as Energy Storage Materials. In *Energy Materials: Structure, Properties and Applications*; Springer: Singapore, 2023; pp. 57–75.
31. Pan, Z.; Chen, H.; Zeng, Y.; et al. *Fluorine Chemistry in Lithium-Ion and Sodium-Ion Batteries*; OAE Publishing Inc.: Alhambra, CA, USA, 2023.
32. Wei, X.; Wang, X.; Tan, X.; et al. Nanostructured conversion-type negative electrode materials for low-cost and high-performance sodium-ion batteries. *Adv. Funct. Mater.* **2018**, *28*, 1804458.
33. Huang, Y.; Zheng, Y.; Li, X.; et al. Electrode materials of sodium-ion batteries toward practical application. *ACS Energy Lett.* **2018**, *3*, 1604–1612.
34. Ma, Y.; Ma, Y.; Bresser, D.; et al. Cobalt disulfide nanoparticles embedded in porous carbonaceous micro-polyhedrons interlinked by carbon nanotubes for superior lithium and sodium storage. *ACS Nano* **2018**, *12*, 7220–7231.
35. Song, Z.; Ma, Y.; Wang, K.; et al. Zinc-regulated hard carbon as a sodium-ion battery anode material. *J. Power Sources* **2025**, *640*, 236798.
36. Wang, J.; Wu, P.; Wang, K.; et al. Composite (bi-) metallic oxides with heterostructure and heteroatom-doped porous carbon as advanced potassium-ion battery anodes. *Batter. Supercaps* **2025**, *8*, e202400779.
37. Li, P.; Shen, Y.; Li, X.; et al. Fullerene-intercalated graphitic carbon nitride as a high-performance anode material for sodium-ion batteries. *Energy Environ. Mater.* **2022**, *5*, 608–616.
38. Hankel, M.; Ye, D.; Wang, L.; et al. Lithium and sodium storage on graphitic carbon nitride. *J. Phys. Chem. C* **2015**, *119*, 21921–21927.
39. Gope, S.; Malunavar, S.; Bhattacharyya, A.J. Li–Ion-Conducting Pillar-Like Graphitic Carbon Nitrides as Novel Anodes for Li–Ion Batteries. *ChemistrySelect* **2018**, *3*, 5364–5376.
40. Liu, D.; Zhang, C.; Zhou, G.; et al. Catalytic effects in lithium–sulfur batteries: Promoted sulfur transformation and reduced shuttle effect. *Adv. Sci.* **2018**, *5*, 1700270.
41. Li, Y.; Li, X.; Zhang, H.; et al. Porous graphitic carbon nitride for solar photocatalytic applications. *Nanoscale Horiz.* **2020**, *5*, 765–786.
42. Wang, L.; Wang, K.; He, T.; et al. Graphitic carbon nitride-based photocatalytic materials: Preparation strategy and application. *ACS Sustain. Chem. Eng.* **2020**, *8*, 16048–16085.
43. Vaya, D.; Kaushik, B.; Surolia, P.K. Recent advances in graphitic carbon nitride semiconductor: Structure, synthesis and applications. *Mater. Sci. Semicond. Process.* **2022**, *137*, 106181.
44. Liang, Q.; Shao, B.; Tong, S.; et al. Recent advances of melamine self-assembled graphitic carbon nitride-based materials: Design, synthesis and application in energy and environment. *Chem. Eng. J.* **2021**, *405*, 126951.
45. Lu, C.; Chen, X. Nanostructure engineering of graphitic carbon nitride for electrochemical applications. *ACS Nano* **2021**, *15*, 18777–18793.
46. Ni, Y.; Wang, R.; Zhang, W.; et al. Graphitic carbon nitride (g-C_3N_4)-based nanostructured materials for photodynamic inactivation: Synthesis, efficacy and mechanism. *Chem. Eng. J.* **2021**, *404*, 126528.
47. Gao, X.; Li, Q.-Y.; Wang, Y.-L.; et al. A facile soft-hard template cooperative organization approach for mesoporous g-C3N4 with high photocatalytic performance. *Appl. Surf. Sci.* **2024**, *657*, 159574.

48. Obregón, S. Exploring nanoengineering strategies for the preparation of graphitic carbon nitride nanostructures. *FlatChem* **2023**, *38*, 100473.
49. Zeng, Y.; Zhan, X.; Li, H.; et al. Bottom-to-Up synthesis of functional carbon nitride polymer: Design principles, controlled synthesis and applications. *Eur. Polym. J.* **2023**, *182*, 111734.
50. Groenewolt, M.; Antonietti, M. Synthesis of g-C_3N_4 nanoparticles in mesoporous silica host matrices. *Adv. Mater.* **2005**, *17*, 1789–1792.
51. Gao, R.; Liao, Q.; Sun, F.; et al. Mesoporous graphitic carbon nitride for photocatalytic coenzyme regeneration. *Microporous Mesoporous Mater.* **2024**, *365*, 112890.
52. Bu, L.; Xie, Q.; Ming, H. Gold nanoparticles decorated three-dimensional porous graphitic carbon nitrides for sensitive anodic stripping voltammetric analysis of trace arsenic (III). *J. Alloys Compd.* **2020**, *823*, 153723.
53. Ajiboye, T.O.; Kuvarega, A.T.; Onwudiwe, D.C. Graphitic carbon nitride-based catalysts and their applications: A review. *Nano-Struct. Nano-Objects* **2020**, *24*, 100577.
54. Xu, Z.; Kong, L.; Wang, H.; et al. Soft-template assisted preparation of hierarchically porous graphitic carbon nitride layers for high-performance supercapacitors. *J. Appl. Polym. Sci.* **2022**, *139*, e52947.
55. Antil, B.; Deka, S. Porous Graphitic Carbon Nitride Nanostructures and Their Application in Photocatalytic Hydrogen Evolution Reaction. *Heterog. Nanocatalysis Energy Environ. Sustain.* **2022**, *1*, 133–163.
56. Wang, H.; Liu, Y.; Kong, L.; et al. Porous graphitic carbon nitride nanosheets with three-dimensional interconnected network as electrode for supercapacitors. *J. Energy Storage* **2023**, *63*, 106935.
57. Li, H.; Wang, L.; Liu, Y.; et al. Mesoporous graphitic carbon nitride materials: Synthesis and modifications. *Res. Chem. Intermed.* **2016**, *42*, 3979–3998.
58. Umekar, M.S.; Bhusari, G.S.; Bhoyar, T.; et al. Graphitic carbon nitride-based photocatalysts for environmental remediation of organic pollutants. *Curr. Nanosci.* **2023**, *19*, 148–169.
59. Nazir, A.; Huo, P.; Rasool, A.T. Recent advances on graphitic carbon nitride-based S-scheme photocatalysts: Synthesis, environmental applications, and challenges. *J. Organomet. Chem.* **2023**, *1004*, 122951.
60. Kailasam, K.; Epping, J.D.; Thomas, A.; et al. Mesoporous carbon nitride–silica composites by a combined sol–gel/thermal condensation approach and their application as photocatalysts. *Energy Environ. Sci.* **2011**, *4*, 4668–4674.
61. Dharani, S.; Gnanasekaran, L.; Arunachalam, S.; et al. Photodegrading Rhodamine B dye with cobalt ferrite-graphitic carbon nitride ($CoFe_2O_4$/g-C_3N_4) composite. *Environ. Res.* **2024**, *258*, 119484.
62. Dharmarajan, N.P.; Vidyasagar, D.; Yang, J.H.; et al. Bio-inspired supramolecular self-assembled carbon nitride nanostructures for photocatalytic water splitting. *Adv. Mater.* **2024**, *36*, 2306895.
63. Asrami, M.R.; Jourshabani, M.; Park, M.H.; et al. A unique and well-designed 2D graphitic carbon nitride with sponge-like architecture for enhanced visible-light photocatalytic activity. *J. Mater. Sci. Technol.* **2023**, *159*, 99–111.
64. Shao, S.; Liu, X.; Wang, R.; et al. Morphologic and microstructural modulation of graphitic carbon nitride through EDTA-2Na mediated supramolecular self-assembly route: Enhanced visible-light-driven photocatalytic activity for antibiotic degradation. *Appl. Surf. Sci.* **2024**, *669*, 160501.
65. Liu, Y.; Guo, X.; Chen, Z.; et al. Microwave-synthesis of g-C3N4 nanoribbons assembled seaweed-like architecture with enhanced photocatalytic property. *Appl. Catal. B Environ.* **2020**, *266*, 118624.
66. Choudhary, P.; Kumar, A.; Krishnan, V. Nanoarchitectonics of phosphorylated graphitic carbon nitride for sustainable, selective and metal-free synthesis of primary amides. *Chem. Eng. J.* **2022**, *431*, 133695.
67. Zheng, T.; Li, M.; Zhou, S.; et al. Gas exfoliation mechanisms of graphitic carbon nitride into few-layered nanosheets. *J. Porous Mater.* **2022**, *29*, 331–340.
68. Attri, P.; Garg, P.; Sharma, P.; et al. Precursor-dependent fabrication of exfoliated graphitic carbon nitride (gCN) for enhanced photocatalytic and antimicrobial activity under visible light irradiation. *J. Clean. Prod.* **2023**, *422*, 138538.
69. Cui, J.; Qi, D.; Wang, X. Research on the techniques of ultrasound-assisted liquid-phase peeling, thermal oxidation peeling and acid-base chemical peeling for ultra-thin graphite carbon nitride nanosheets. *Ultrason. Sonochem.* **2018**, *48*, 181–187.
70. Zou, X.; Zhao, Y.; Li, M.; et al. Construction of graphitic carbon nitride nanosheets via an improved solvent exfoliation strategy and interfacial mechanics insight from molecular dynamics simulations. *J. Porous Mater.* **2021**, *28*, 943–954.
71. Gowri, V.M.; Ajith, A.; John, S.A. Systematic study on morphological, electrochemical impedance, and electrocatalytic activity of graphitic carbon nitride modified on a glassy carbon substrate from sequential exfoliation in water. *Langmuir* **2021**, *37*, 10538–10546.
72. Nguyen, M.D.; Nguyen, T.B.; Thamilselvan, A.; et al. Fabrication of visible-light-driven tubular F, P-codoped graphitic carbon nitride for enhanced photocatalytic degradation of tetracycline. *J. Environ. Chem. Eng.* **2022**, *10*, 106905.
73. Yang, S.; Li, H.; Li, H.; et al. Rational design of 3D carbon nitrides assemblies with tunable nano-building blocks for efficient visible-light photocatalytic CO_2 conversion. *Appl. Catal. B Environ.* **2022**, *316*, 121612.
74. Lopes, P.P.; Stamenkovic, V.R. Past, present, and future of lead–acid batteries. *Science* **2020**, *369*, 923–924.

75. Scrosati, B. History of lithium batteries. *J. Solid State Electrochem.* **2011**, *15*, 1623–1630.
76. Tsais, P.-J.; Chan, L. Nickel-based batteries: Materials and chemistry. *Electr. Transm. Distrib. Storage Syst.* **2013**, 309–397. https://doi.org/10.1533/9780857097378.3.309.
77. Kurtulmuş, Z.N.; Karakaya, A. Review of lithium-ion, fuel cell, sodium-beta, nickel-based and metal-air battery technologies used in electric vehicles. *Int. J. Energy Appl. Technol.* **2023**, *10*, 103–113.
78. Sato, Y.; Takeuchi, S.; Kobayakawa, K. Cause of the memory effect observed in alkaline secondary batteries using nickel electrode. *J. Power Sources* **2001**, *93*, 20–24.
79. Arun, V.; Kannan, R.; Ramesh, S.; et al. Review on Li-Ion Battery vs Nickel Metal Hydride Battery in EV. *Adv. Mater. Sci. Eng.* **2022**, *2022*, 7910072.
80. Shin, J.; Choi, J.W. Opportunities and reality of aqueous rechargeable batteries. *Adv. Energy Mater.* **2020**, *10*, 2001386.
81. Zhang, X.; Lou, Z.; Gao, M.; et al. Metal Hydrides for Advanced Hydrogen/Lithium Storage and Ionic Conduction Applications. *Acc. Mater. Res.* **2024**, *5*, 371–384.
82. Armand, M.; Axmann, P.; Bresser, D.; et al. Lithium-ion batteries–Current state of the art and anticipated developments. *J. Power Sources* **2020**, *479*, 228708.
83. Jetybayeva, A.; Aaron, D.S.; Belharouak, I.; et al. Critical review on recently developed lithium and non-lithium anode-based solid-state lithium-ion batteries. *J. Power Sources* **2023**, *566*, 232914.
84. Deng, H.; Aifantis, K.E. Applications of lithium batteries. *Recharg. Ion Batter. Mater. Des. Appl. Li-Ion Cells Beyond* **2023**, 83–103. https://doi.org/10.1002/9783527836703.ch4.
85. Michelini, E.; Höschele, P.; Ratz, F.; et al. Potential and most promising second-life applications for automotive lithium-ion batteries considering technical, economic and legal aspects. *Energies* **2023**, *16*, 2830.
86. Stampatori, D.; Raimondi, P.P.; Noussan, M. Li-ion batteries: A review of a key technology for transport decarbonization. *Energies* **2020**, *13*, 2638.
87. Bones, R.; Teagle, D.; Brooker, S.; et al. Development of a Ni, NiCl2 positive electrode for a liquid sodium (ZEBRA) battery cell. *J. Electrochem. Soc.* **1989**, *136*, 1274.
88. Oshima, T.; Kajita, M.; Okuno, A. Development of sodium-sulfur batteries. *Int. J. Appl. Ceram. Technol.* **2004**, *1*, 269–276.
89. Dustmann, C.-H. Advances in ZEBRA batteries. *J. Power Sources* **2004**, *127*, 85–92.
90. Yang, H.; Zhang, Q.; Chen, M.; et al. Unveiling the origin of air stability in polyanion and layered-oxide cathode materials for sodium-ion batteries and their practical application considerations. *Adv. Funct. Mater.* **2024**, *34*, 2308257.
91. Yabuuchi, N.; Kubota, K.; Dahbi, M.; et al. Research development on sodium-ion batteries. *Chem. Rev.* **2014**, *114*, 11636–11682.
92. Perveen, T.; Siddiq, M.; Shahzad, N.; et al. Prospects in anode materials for sodium ion batteries-A review. *Renew. Sustain. Energy Rev.* **2020**, *119*, 109549.
93. Jan, W.; Khan, A.D.; Iftikhar, F.J.; et al. Recent advancements and challenges in deploying lithium sulfur batteries as economical energy storage devices. *J. Energy Storage* **2023**, *72*, 108559.
94. Prajapati, A.K.; Bhatnagar, A. A review on anode materials for lithium/sodium-ion batteries. *J. Energy Chem.* **2023**, *83*, 509–540.
95. Chen, Y.; Wang, T.; Tian, H.; et al. Advances in lithium–sulfur batteries: From academic research to commercial viability. *Adv. Mater.* **2021**, *33*, 2003666.
96. Chen, J.; Mao, Z.; Zhang, L.; et al. Nitrogen-deficient graphitic carbon nitride with enhanced performance for lithium ion battery anodes. *ACS Nano* **2017**, *11*, 12650–12657.
97. Li, D.; Liu, J.; Wang, W.; et al. Synthesis of porous N deficient graphitic carbon nitride and utilization in lithium-sulfur battery. *Appl. Surf. Sci.* **2021**, *569*, 151058.
98. Liang, Y.; Zhao, C.Z.; Yuan, H.; et al. A review of rechargeable batteries for portable electronic devices. *InfoMat* **2019**, *1*, 6–32.
99. Kawahara, Y.; Sakabe, K.; Nakao, R.; et al. Development of status detection method of lithium-ion rechargeable battery for hybrid electric vehicles. *J. Power Sources* **2021**, *481*, 228760.
100. Newaskar, D.; Patil, B. Batteries for Active Implantable Medical Devices. In Proceedings of the 2021 International Conference on Intelligent Technologies (CONIT), Hubli, India, 25–27 June 2021; pp. 1–7.
101. Schipper, F.; Aurbach, D. A brief review: Past, present and future of lithium ion batteries. *Russ. J. Electrochem.* **2016**, *52*, 1095–1121.
102. Zhao, L.; Zhang, T.; Li, W.; et al. Engineering of sodium-ion batteries: Opportunities and challenges. *Engineering* **2023**, *24*, 172–183.
103. Asmare, M.; Zegeye, M.; Ketema, A. Advancement of electrically rechargeable metal-air batteries for future mobility. *Energy Rep.* **2024**, *11*, 1199–1211.
104. Lv, Z.-C.; Wang, P.-F.; Wang, J.-C.; et al. Key challenges, recent advances and future perspectives of rechargeable lithium-sulfur batteries. *J. Ind. Eng. Chem.* **2023**, *124*, 68–88.

105. Nakamura, N.; Ahn, S.; Momma, T.; et al. Future potential for lithium-sulfur batteries. *J. Power Sources* **2023**, *558*, 232566.
106. Fichtner, M.; Edström, K.; Ayerbe, E.; et al. Rechargeable batteries of the future—The state of the art from a BATTERY 2030+ perspective. *Adv. Energy Mater.* **2022**, *12*, 2102904.
107. Hasa, I.; Mariyappan, S.; Saurel, D.; et al. Challenges of today for Na-based batteries of the future: From materials to cell metrics. *J. Power Sources* **2021**, *482*, 228872.
108. Ming, F.; Liang, H.; Huang, G.; et al. MXenes for rechargeable batteries beyond the lithium-ion. *Adv. Mater.* **2021**, *33*, 2004039.
109. Tang, X.; Liu, C.; Wang, H.; et al. Pristine metal-organic frameworks for next-generation batteries. *Coord. Chem. Rev.* **2023**, *494*, 215361.
110. Zhang, H.; Yang, Y.; Ren, D.; et al. Graphite as anode materials: Fundamental mechanism, recent progress and advances. *Energy Storage Mater.* **2021**, *36*, 147–170.
111. Zhang, Z.; Fang, Z.; Xiang, Y.; et al. Cellulose-based material in lithium-sulfur batteries: A review. *Carbohydr. Polym.* **2021**, *255*, 117469.
112. Li, S.; Fan, Z. Encapsulation methods of sulfur particles for lithium-sulfur batteries: A review. *Energy Storage Mater.* **2021**, *34*, 107–127.
113. Fan, K.; Huang, H. Two-Dimensional Host Materials for Lithium-Sulfur Batteries: A Review and Perspective. *Energy Storage Mater.* **2022**, *50*, 696–717.
114. Lai, Y.; Nie, H.; Xu, X.; et al. Interfacial Molecule Mediators in Cathodes for Advanced Li–S Batteries. *ACS Appl. Mater. Interfaces* **2019**, *11*, 29978–29984.
115. Ponnada, S.; Kiai, M.S.; Gorle, D.B.; et al. History and recent developments in divergent electrolytes towards high-efficiency lithium–sulfur batteries–a review. *Mater. Adv.* **2021**, *2*, 4115–4139.
116. Yang, L.; Li, Q.; Wang, Y.; et al. A review of cathode materials in lithium-sulfur batteries. *Ionics* **2020**, *26*, 5299–5318.
117. Wang, J.; Han, W.Q. A review of heteroatom doped materials for advanced lithium–sulfur batteries. *Adv. Funct. Mater.* **2022**, *32*, 2107166.
118. Liao, K.; Mao, P.; Li, N.; et al. Stabilization of polysulfides via lithium bonds for Li–S batteries. *J. Mater. Chem. A* **2016**, *4*, 5406–5409.
119. Zhang, J.; Li, J.Y.; Wang, W.P.; et al. Microemulsion Assisted Assembly of 3D Porous S/Graphene@ g-C_3N_4 Hybrid Sponge as Free-Standing Cathodes for High Energy Density Li–S Batteries. *Adv. Energy Mater.* **2018**, *8*, 1702839.
120. Du, M.; Tian, X.; Ran, R.; et al. Tuning nitrogen in graphitic carbon nitride enabling enhanced performance for polysulfide confinement in Li–S batteries. *Energy Fuels* **2020**, *34*, 11557–11564.
121. Fan, C.-Y.; Yuan, H.-Y.; Li, H.-H.; et al. The effective design of a polysulfide-trapped separator at the molecular level for high energy density Li–S batteries. *ACS Appl. Mater. Interfaces* **2016**, *8*, 16108–16115.
122. Ding, L.; Lu, Q.; Permana, A.D.C.; et al. Oxygen-Doped Carbon Nitride Tubes for Highly Stable Lithium–Sulfur Batteries. *Energy Technol.* **2021**, *9*, 2001057.
123. Jun, Y.S.; Lee, E.Z.; Wang, X.; et al. From melamine-cyanuric acid supramolecular aggregates to carbon nitride hollow spheres. *Adv. Funct. Mater.* **2013**, *23*, 3661–3667.
124. He, W.; He, X.; Du, M.; et al. Three-dimensional functionalized carbon nanotubes/graphitic carbon nitride hybrid composite as the sulfur host for high-performance lithium–sulfur batteries. *J. Phys. Chem. C* **2019**, *123*, 15924–15934.
125. Hong, X.; Liu, Y.; Fu, J.; et al. A wheat flour derived hierarchical porous carbon/graphitic carbon nitride composite for high-performance lithium–sulfur batteries. *Carbon* **2020**, *170*, 119–126.
126. Song, J.; Feng, S.; Zhu, C.; et al. Tuning the structure and composition of graphite-phase polymeric carbon nitride/reduced graphene oxide composites towards enhanced lithium-sulfur batteries performance. *Electrochim. Acta* **2017**, *248*, 541–546.
127. He, F.; Li, K.; Yin, C.; et al. A combined theoretical and experimental study on the oxygenated graphitic carbon nitride as a promising sulfur host for lithium–sulfur batteries. *J. Power Sources* **2018**, *373*, 31–39.
128. Ma, H.; Liu, X.; Liu, N.; et al. Defect-rich porous tubular graphitic carbon nitride with strong adsorption towards lithium polysulfides for high-performance lithium-sulfur batteries. *J. Mater. Sci. Technol.* **2022**, *115*, 140–147.
129. Ma, H.; Song, C.; Liu, N.; et al. Nitrogen-Deficient Graphitic Carbon Nitride/Carbon Nanotube as Polysulfide Barrier of High-Performance Lithium-Sulfur Batteries. *ChemElectroChem* **2020**, *7*, 4906–4912.
130. Li, C.; Gao, K.; Zhang, Z. Graphitic carbon nitride as polysulfide anchor and barrier for improved lithium–sulfur batteries. *Nanotechnology* **2018**, *29*, 465401.
131. Chung, S.H.; Manthiram, A. Current status and future prospects of metal–sulfur batteries. *Adv. Mater.* **2019**, *31*, 1901125.
132. Pan, Z.; Brett, D.J.; He, G.; et al. Progress and perspectives of organosulfur for lithium–sulfur batteries. *Adv. Energy Mater.* **2022**, *12*, 2103483.

133. Zhao, X.; Wang, P.; Lv, E.; et al. Screening MXenes for novel anode material of lithium-ion batteries with high capacity and stability: A DFT calculation. *Appl. Surf. Sci.* **2021**, *569*, 151050.
134. Goodenough, J.B.; Park, K.-S. The Li-ion rechargeable battery: A perspective. *J. Am. Chem. Soc.* **2013**, *135*, 1167–1176.
135. Deifallah, M.; McMillan, P.F.; Corà, F. Electronic and structural properties of two-dimensional carbon nitride graphenes. *J. Phys. Chem. C* **2008**, *112*, 5447–5453.
136. Veith, G.M.; Baggetto, L.; Adamczyk, L.A.; et al. Electrochemical and solid-state lithiation of graphitic C3N4. *Chem. Mater.* **2013**, *25*, 503–508.
137. Zhang, W.; Yin, J.; Chen, C.; et al. Carbon nitride derived nitrogen-doped carbon nanosheets for high-rate lithium-ion storage. *Chem. Eng. Sci.* **2021**, *241*, 116709.
138. Olabi, A.G.; Abdelkareem, M.A.; Wilberforce, T.; et al. Application of graphene in energy storage device–A review. *Renew. Sustain. Energy Rev.* **2021**, *135*, 110026.
139. Fang, S.; Bresser, D.; Passerini, S. Transition metal oxide anodes for electrochemical energy storage in lithium-and sodium-ion batteries. *Transit. Met. Oxides Electrochem. Energy Storage* **2022**, 55–99. https://doi.org/10.1002/9783527817252.ch4.
140. Joshi, B.; Samuel, E.; Kim, T.-G.; et al. Supersonically spray-coated zinc ferrite/graphitic-carbon nitride composite as a stable high-capacity anode material for lithium-ion batteries. *J. Alloys Compd.* **2018**, *768*, 525–534.
141. Tao, H.; Xiong, L.; Du, S.; et al. Interwoven N and P dual-doped hollow carbon fibers/graphitic carbon nitride: An ultrahigh capacity and rate anode for Li and Na ion batteries. *Carbon* **2017**, *122*, 54–63.
142. Subramaniyam, C.M.; Deshmukh, K.A.; Tai, Z.; et al. 2D layered graphitic carbon nitride sandwiched with reduced graphene oxide as nanoarchitectured anode for highly stable lithium-ion battery. *Electrochim. Acta* **2017**, *237*, 69–77.
143. Yuan, Z.; Hu, Z.; Gao, P.; et al. Graphitic carbon nitride-derived high lithium storage capacity graphite material with regular layer structure and the structural evolution mechanism. *Electrochim. Acta* **2022**, *409*, 139985.
144. Dutta, D.P.; Pathak, D.D.; Abraham, S.; et al. An insight into the sodium-ion and lithium-ion storage properties of CuS/graphitic carbon nitride nanocomposite. *RSC Adv.* **2022**, *12*, 12383–12395.
145. Li, Q.; Yang, D.; Chen, H.; et al. Advances in metal phosphides for sodium-ion batteries. *SusMat* **2021**, *1*, 359–392.
146. Wang, J.; Yue, X.; Xie, Z.; et al. MOFs-derived transition metal sulfide composites for advanced sodium ion batteries. *Energy Storage Mater.* **2021**, *41*, 404–426.
147. Tan, H.; Feng, Y.; Rui, X.; et al. Metal chalcogenides: Paving the way for high-performance sodium/potassium-ion batteries. *Small Methods* **2020**, *4*, 1900563.
148. Karuppasamy, K.; Lin, J.; Vikraman, D.; et al. Towards greener energy storage: Brief insights into 3D printed anode materials for sodium-ion batteries. *Curr. Opin. Electrochem.* **2024**, *45*, 101482.
149. Goikolea, E.; Palomares, V.; Wang, S.; et al. Na-ion batteries—Approaching old and new challenges. *Adv. Energy Mater.* **2020**, *10*, 2002055.
150. Rudola, A.; Rennie, A.J.; Heap, R.; et al. Commercialisation of high energy density sodium-ion batteries: Faradion's journey and outlook. *J. Mater. Chem. A* **2021**, *9*, 8279–8302.
151. Das, H.T.; Babu, S.P.; Mondal, A.; et al. 2D-layered graphitic carbon nitride nanosheets for electrochemical energy storage applications. *J. Power Sources* **2024**, *603*, 234374.
152. Haruna, A.; Dönmez, K.B.; Hooshmand, S.; et al. Harmony of nanosystems: Graphitic carbon nitride/carbon nanomaterial hybrid architectures for energy storage in supercapacitors and batteries. *Carbon* **2024**, *226*, 119177.
153. Thomas, S.A.; Pallavolu, M.R.; Khan, M.E.; et al. Graphitic carbon nitride (g-C_3N_4): Futuristic material for rechargeable batteries. *J. Energy Storage* **2023**, *68*, 107673.
154. Zhou, P.; Hou, L.; Song, T.; et al. Tuning N-species of graphitic carbon nitride for high-performance anode in sodium ion battery. *ACS Appl. Energy Mater.* **2022**, *5*, 9286–9291.
155. Cha, W.; Kim, I.Y.; Lee, J.M.; et al. Sulfur-doped mesoporous carbon nitride with an ordered porous structure for sodium-ion batteries. *ACS Appl. Mater. Interfaces* **2019**, *11*, 27192–27199.
156. Wang, Y.; Li, H.; Di, S.; et al. Constructing long-cycling crystalline C3N4-based carbonaceous anodes for sodium-ion battery via N configuration control. *Carbon Energy* **2024**, *6*, e388.
157. Zhou, Y.; Zhang, S.; Xu, J.; et al. Construction of MoS2-nitrogen-deficient graphitic carbon nitride anode toward high performance Sodium-ions batteries. *Mater. Lett.* **2020**, *273*, 127890.
158. Yang, J.; Liu, Z.; Sheng, X.; et al. Tin nanoparticle in-situ decorated on nitrogen-deficient carbon nitride with excellent sodium storage performance. *J. Colloid Interface Sci.* **2022**, *624*, 40–50.
159. Zhang, W.; Sun, M.; Yin, J.; et al. Rational design of carbon anodes by catalytic pyrolysis of graphitic carbon nitride for efficient storage of Na and K mobile ions. *Nano Energy* **2021**, *87*, 106184.
160. Patel, A.; Gupta, H.; Singh, S.K.; et al. Superior cycling stability of saturated graphitic carbon nitride in hydrogel reduced graphene oxide anode for Sodium-ion battery. *FlatChem* **2022**, *33*, 100351.
161. Weng, G.M.; Xie, Y.; Wang, H.; et al. A promising carbon/g-C3N4 composite negative electrode for a long-life sodium-ion battery. *Angew. Chem.* **2019**, *131*, 13865–13871.

162. Song, J.; Maulana, A.Y.; Kim, H.; et al. N-doped Graphitic Carbon Coated Fe_2O_3 Using Dopamine as an Anode Material for Sodium-Ion Batteries. *J. Alloys Compd.* **2022**, *921*, 166082.
163. Nazir, G.; Rehman, A.; Lee, J.-H.; et al. A Review of Rechargeable Zinc–Air Batteries: Recent Progress and Future Perspectives. *Nano-Micro Lett.* **2024**, *16*, 138.
164. Bi, X.; Jiang, Y.; Chen, R.; et al. Rechargeable zinc–air versus lithium–air battery: From fundamental promises toward technological potentials. *Adv. Energy Mater.* **2024**, *14*, 2302388.
165. Yu, H.; Lv, C.; Yan, C.; et al. Interface engineering for aqueous aluminum metal batteries: Current progresses and future prospects. *Small Methods* **2024**, *8*, 2300758.
166. Wang, T.; Yang, T.; Luo, D.; et al. High-Energy-Density Solid-State Metal–Air Batteries: Progress, Challenges, and Perspectives. *Small* **2024**, *20*, 2309306.
167. Cao, R.; Lee, J.S.; Liu, M.; et al. Recent progress in non-precious catalysts for metal-air batteries. *Adv. Energy Mater.* **2012**, *2*, 816–829.
168. Liu, Q.; Pan, Z.; Wang, E.; et al. Aqueous metal-air batteries: Fundamentals and applications. *Energy Storage Mater.* **2020**, *27*, 478–505.
169. Li, T.; Huang, M.; Bai, X.; et al. Metal–air batteries: A review on current status and future applications. *Prog. Nat. Sci. Mater. Int.* **2023**, *33*, 151–171.
170. Lyth, S.M.; Nabae, Y.; Islam, N.M.; et al. Electrochemical oxygen reduction on carbon nitride. *ECS Trans.* **2010**, *28*, 11.
171. Gong, X.-F.; Zhang, Y.-L.; Zhao, L.; et al. Zinc/graphitic carbon nitride co-mediated dual-template synthesis of densely populated Fe–N x-embedded 2D carbon nanosheets towards oxygen reduction reactions for Zn–air batteries. *J. Mater. Chem. A* **2022**, *10*, 5971–5980.
172. Tang, W.; Teng, K.; Guo, W.; et al. Defect-engineered Co_3O_4@ nitrogen-deficient graphitic carbon nitride as an efficient bifunctional electrocatalyst for high-performance metal-air batteries. *Small* **2022**, *18*, 2202194.
173. Niu, W.; Marcus, K.; Zhou, L.; et al. Enhancing electron transfer and electrocatalytic activity on crystalline carbon-conjugated g-C3N4. *ACS Catal.* **2018**, *8*, 1926–1931.
174. Shinde, S.S.; Lee, C.-H.; Sami, A.; et al. Scalable 3-D carbon nitride sponge as an efficient metal-free bifunctional oxygen electrocatalyst for rechargeable Zn–air batteries. *Acs Nano* **2017**, *11*, 347–357.
175. Kumar, S.; Jena, A.; Hu, Y.C.; et al. Cobalt diselenide nanorods grafted on graphitic carbon nitride: A synergistic catalyst for oxygen reactions in rechargeable Li− O2 batteries. *ChemElectroChem* **2018**, *5*, 29–35.
176. Shinde, S.S.; Yu, J.-Y.; Song, J.-W.; et al. Highly active and durable carbon nitride fibers as metal-free bifunctional oxygen electrodes for flexible Zn–air batteries. *Nanoscale Horiz.* **2017**, *2*, 333–341.
177. Wu, L.; Zhang, Y.; Shang, P.; et al. Redistributing Zn ion flux by bifunctional graphitic carbon nitride nanosheets for dendrite-free zinc metal anodes. *J. Mater. Chem. A* **2021**, *9*, 27408–27414.
178. Li, P.; Wang, H.; Tan, X.; et al. Bifunctional electrocatalyst with CoN_3 active sties dispersed on N-doped graphitic carbon nanosheets for ultrastable Zn-air batteries. *Appl. Catal. B Environ.* **2022**, *316*, 121674.